https://doi.org/10.5194/egusphere-2025-4450
Preprint. Discussion started: 18 September 2025

Towards a semi-asynchronous method for hydrological modeling in climate change studies

Frédéric Talbot[1], Simon Ricard[2], Guillaume Drolet[3], Annie Poulin[1], Jean-Luc Martel[1], Richard Arsenault[1], Jean-Daniel Sylvain[1,3]

[1] Hydrology, Climate and Climate Change Laboratory, École de technologie supérieure, Université du Québec, Montréal, H3C 1K3, Canada
[2] Sciences and Engineering, Université Laval, Québec, G1V 0A6, Canada
[3] Direction de la recherche forestière, Ministère des Ressources naturelles et des Forêts, Québec, G1P 3W8, Canada

Correspondence to: Frédéric Talbot (frederic.talbot.2@ens.etsmtl.ca)

Abstract. Hydrological impact assessments under climate change commonly rely on conventional modeling chains where climate projections are bias-corrected before being used in hydrological simulations. While this improves agreement with historical observations, it can introduce methodological uncertainties, reduce the diversity of climate ensembles, and smooth out extreme events. Asynchronous methods have been proposed as an alternative, allowing hydrological models to be calibrated directly with raw climate model outputs. However, fully asynchronous methods often fail to capture the timing of key hydrological processes, especially in snow-affected regions.

This study introduces and evaluates a semi-asynchronous calibration approach that incorporates a monthly temporal structure to address these limitations. Using the physically based WaSiM model, we compare the semi-asynchronous, fully asynchronous, and conventional methods across ten snow-influenced catchments in southern Quebec, Canada, under historical and future climate conditions.

The results show that while the fully asynchronous and semi-asynchronous methods perform well in preserving streamflow distributions and high-flow extremes, only the semi-asynchronous method succeeds in restoring the seasonal timing of key processes such as snowmelt and low flows. The semi-asynchronous method notably reduces intermodel variability in streamflow and snow water equivalent compared to the fully asynchronous approach. It also exhibits seasonal dynamics that closely align with observations and the conventional method, despite relying on uncorrected climate inputs. In contrast, the fully asynchronous method shows signs of desynchronization, with unrealistic snowmelt timing and elevated variability across projections. The conventional method, while more stable in the historical period, exhibits an increase in intermodel variability under future conditions, likely due to divergent magnitudes of projected change across climate models. The semi-asynchronous method presents a clear improvement over the fully asynchronous approach by restoring temporal coherence and improving the simulation of seasonal processes. It also reduces intermodel variability while maintaining the raw climate signal and preserving the distribution of streamflow.

Compared to the conventional method, which benefits from stable and consistent simulations but tends to dampen extremes through bias correction, the semi-asynchronous approach offers a compelling alternative. It strikes a different balance between

https://doi.org/10.5194/egusphere-2025-4450
Preprint. Discussion started: 18 September 2025

realism, ensemble diversity, and the ability to represent extreme events, making it particularly valuable for future-oriented climate impact assessments.

This study highlights the potential of the semi-asynchronous method as an innovative and robust tool for hydrological modeling under climate change. As climate model simulations continue to improve and their biases are progressively reduced, the semi-asynchronous approach is poised to benefit significantly, enhancing its potential for future hydrological projections.

1 Introduction

Climate change is one of the most significant challenges of our time, with profound implications for the Earth's hydrological systems. Alterations in temperature and precipitation regimes affect water availability and the timing of hydrological events. Understanding these impacts is crucial for effective water resource management and decision-making (Arsenault et al., 2013; Calvin et al., 2023). Accurate climate change studies are essential for developing strategies to mitigate and adapt to these changes, ensuring the sustainability of natural resources and the resilience of human and ecological systems (Milly et al., 2005; Sivakumar, 2011).

The complex dynamics of watersheds require hydrological models capable of precisely simulating both surface and subsurface processes (Farjad et al., 2016; T. W. Chu and A. Shirmohammadi, 2004). Accurate depiction of these processes within hydrological models is essential for assessing the impacts of climate change (Kour *et al.*, 2016). Physically based and spatially distributed hydrological models, such as the Water Balance Simulation Model (WaSiM) (Schulla, 2021), are particularly valuable due to their detailed representation of key processes including surface runoff, groundwater recharge, interflow, and baseflow. These models further enable accurate simulation of hydroclimatic variables, which are essential for understanding the physical processes driving water flow and distribution within a catchment (Bormann and Elfert, 2010; Förster et al., 2017, 2018; Jasper et al., 2006; Natkhin et al., 2012). The use of physically based models like WaSiM, which capture local heterogeneity and finer-scale processes, provides a robust framework for evaluating climate change impacts on hydrology (Devia et al., 2015; Ludwig et al., 2009; Poulin et al., 2011) and supports stakeholders in making decisions that are both data-driven and aligned with strategic goals.

The conventional method for evaluating climate change impacts on hydrology involves a multi-step modeling chain designed to mitigate biases in both the hydrological model and the climate data. The method typically starts with the calibration of a hydrological model using observed meteorological data. Subsequently, raw climate model outputs are corrected using techniques such as quantile mapping (Themeßl et al., 2011; Mpelasoka and Chiew, 2009) to reduce potential biases with respect to the observed meteorological data. The calibrated hydrological model is then driven by these bias-corrected climate data to simulate hydrological processes over both a reference and a future period. By comparing the differences between these two periods, the method estimates the potential effects of climate change on hydroclimatic variables, enabling a clearer understanding of how projected climate change will influence key hydrological processes.

https://doi.org/10.5194/egusphere-2025-4450
Preprint. Discussion started: 18 September 2025

While widely used, conventional methods are constrained by both technical and subjective considerations, including modeling assumptions and methodological choices that can introduce uncertainty in the modeling chain (Moges et al., 2021). Bias correction can disrupt the physical consistency between simulated climate variables and affect long-term climate change signals (Chen et al., 2021; Lee et al., 2019). Advanced techniques, such as multivariate quantile mapping bias correction (MBCn) (Cannon, 2018), have been developed to address some of these issues while preserving inter-variable relationships, which are essential for reliable hydrological modeling. Additionally, the choice of bias correction method itself contributes to overall uncertainty in hydrological projections, as studies have shown that different correction techniques can alter streamflow estimates and influence the magnitude of projected hydrological impacts (Senatore et al., 2022; Chae and Chung, 2024). Chen et al. (2021) further highlight the challenges of maintaining the integrity of climate signals due to the non-stationarity of biases in climate model outputs over time. Their study, which compares pre-processing bias correction of climate model outputs with post-processing corrections applied directly to hydrological model outputs, reveals that while both approaches can significantly reduce biases, they also introduce uncertainties, particularly when dealing with sharp seasonal gradients in correction factors. Despite these challenges, they recommend using a pre-processing approach rather than post-processing for climate impact studies. Additionally, conventional methods rely on high-quality meteorological observations, which are often unavailable in many regions (Ricard et al., 2023).

Asynchronous methods have been proposed to address some of these challenges (Ricard et al., 2019, 2020, 2023; Valencia Giraldo et al., 2023). This framework avoids the need for bias correction by adapting the hydrological model calibration process to directly use raw climate model projection data. This allows conducting climate change studies without relying on observed meteorological data or the underlying assumptions of conventional methods, albeit at the cost of reduced temporal synchronicity. Because the sequence of climatic events within climate model simulations is different from the historical observations, it is not possible to use the correlation between observed and simulated daily streamflow during the calibration process. Instead, the fully asynchronous method focuses on calibrating the statistical distribution of observed streamflow rather than reproducing historical time series. Given that most climate change impact studies assess the projected change in statistical properties between a reference and a future period (Piani et al., 2010), the need for accurate daily temporal correlation may become less critical (Ricard et al., 2019).

While fully asynchronous methods offer a promising alternative to conventional modeling chains by preserving the raw climate signal and streamflow distribution, they might do so at the expense of temporal coherence in hydrological processes. This study introduces a semi-asynchronous method that seeks to overcome this possible limitation by incorporating a monthly calibration structure, thereby restoring seasonal alignment without relying on bias correction. Using the physically based WaSiM model, the study evaluates and compares the conventional, fully asynchronous, and semi-asynchronous methods across ten snow-influenced catchments in southern Quebec. The objective is to assess how each approach represents key hydroclimatic variables and seasonal processes under both historical and future climate conditions. The semi-asynchronous method emerges as a compelling compromise, retaining the advantages of the fully asynchronous framework while significantly improving temporal realism and reducing intermodel variability. This comparison provides valuable insights into

https://doi.org/10.5194/egusphere-2025-4450
Preprint. Discussion started: 18 September 2025

the trade-offs between methodological simplicity, process fidelity, and ensemble diversity in hydrological climate change impact assessments.

2 Methods and data

2.1 Study area

The study focuses on a selection of forested catchments in Southern Quebec, Canada, chosen for their varied sizes and hydrological characteristics. These catchments range in area from 549 km² to 1910 km² (Table 1), providing a diverse representation of the region's physiographic and climatic conditions (Fig. 1). This subset was selected from catchments previously studied (Talbot et al., 2025), where we have extensive knowledge of their behavior and a well-established baseline for comparison. These catchments are well-suited for hydrological modeling with WaSiM, as their natural hydrological processes remain largely intact and are minimally influenced by human-made structures such as dams. The availability of comprehensive streamflow data further supports their suitability for this study.

The region experiences a humid continental climate, with significant seasonal variation characterized by cold, snowy winters and warm, rainy summers. The Köppen-Geiger Climate Classification designates most of this region as Dfb (Humid Continental Mild Summer Wet All Year), with a smaller northern part classified as Dfc (Subarctic with Cool Summers and Year-round Precipitation) (Beck et al., 2018). Specifically, the Godbout, Matane, and Bonaventure catchments belong to the Dfc climate class, while all other catchments fall under the Dfb classification.

Climatic conditions show marked seasonal variations. Winters, extending from December to February, are cold with significant snowfall, contributing to the snowpack that influences spring runoff. Average temperatures during these months frequently drop below freezing, and snow depths can accumulate substantially, impacting streamflow upon melting.

Summers, from June to August, are characterized by warm temperatures and increased rainfall (Fig. 6). The transitional seasons of spring (March to May) and autumn (September to November) exhibit moderate temperatures and variable precipitation, playing a significant role in the hydrological cycle by contributing to groundwater recharge and streamflow variability.

Table 1. Physical and meteorological characteristics of the selected catchments in Southern Quebec.

Catchments	Area (km^2)	Mean Elevation (m)	Dominant Soil Type	Dominant Land Use	Annual Rainfall [a] (mm)	Annual Snowfall [a] (mm)	Annual Runoff (mm)
Bonaventure	1910	356	Sandy Loam	Coniferous forest	753	446	675
Matane	1650	284	Sandy Loam	Mixed forest	789	480	722
Ouelle	795	315	Sandy Loam	Mixed forest	826	424	604
Bécancour	919	305	Sandy Loam	Deciduous forest	1011	389	743
Nicolet S-O	549	259	Sandy Loam	Cropland	1057	341	719

https://doi.org/10.5194/egusphere-2025-4450
Preprint. Discussion started: 18 September 2025

Au Saumon	738	465	Loam	Deciduous forest	935	446	810
Bras du Nord	642	511	Sandy Loam	Mixed forest	1034	444	952
Du Loup	774	381	Sandy Loam	Mixed forest	795	355	504
Valin	746	441	Sandy Loam	Mixed forest	922	436	988
Godbout	1570	302	Sandy Loam	Coniferous forest	732	434	822

[a] Values are derived from WaSiM simulations (1981–2020) using ERA5 data downscaled to 1000 m × 1000 m. Values represent the average across all catchment pixels.

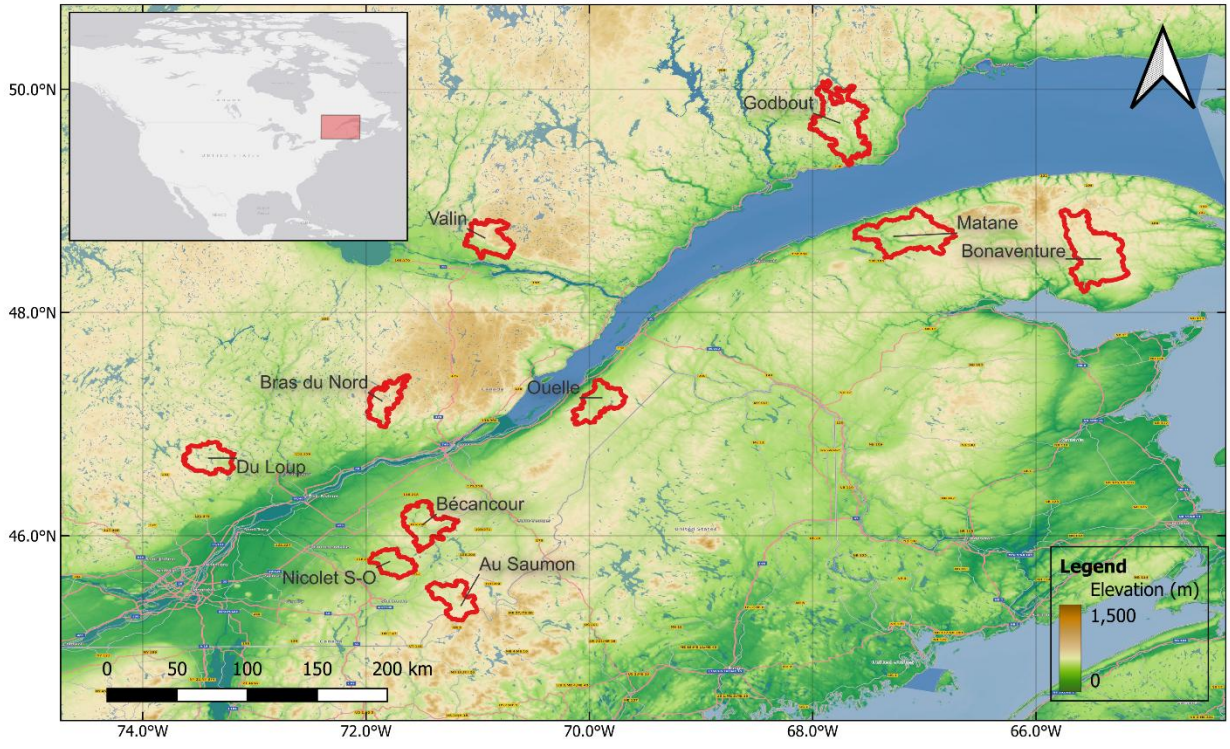

Figure 1. Locations of the selected catchments within Southern Quebec, Canada, outlined in red. The inset map provides the location of the study area within North America.

2.2 Data

2.2.1 Hydrometeorological data

This study utilizes daily total precipitation and mean temperature data from the ECMWF Reanalysis v5 (ERA5) (Hersbach et al., 2020) for the period 1981 to 2020. ERA5 was chosen due to its advanced features over previous reanalysis datasets, such as finer spatial resolution, hourly time step, and a more sophisticated data assimilation system that incorporates a wider range

https://doi.org/10.5194/egusphere-2025-4450
Preprint. Discussion started: 18 September 2025

of observational inputs. These features make ERA5 a suitable reference dataset for hydrological modeling, as demonstrated in Tarek *et al.* (2020), where ERA5-based hydrological simulations performed equivalently to observational data in most regions, including our study area. Additionally, ERA5 showed reduced biases in temperature and precipitation compared to the ERA-Interim dataset, further justifying its use as a reliable and accurate source of climate data for climate change studies. While ERA5-Land offers finer resolution, ERA5 was deemed sufficient for this study since the region is not mountainous, and the focus is on long-term trends rather than specific events. The coarser resolution of ERA5 (31 km) still provides multiple grid points per catchment, allowing interpolation to match the model's resolution, making it an appropriate choice for our analysis. Streamflow data was sourced from the *Hydroclimatic Atlas of Southern Québec* (MDDELCC, 2022), covering the period from 1981 to 2010. This dataset provides daily measurements, though some catchments have minor gaps, primarily during winter months due to ice cover and ice jams. These periods were excluded from model calibration and analyses to maintain data accuracy.

2.2.2 Elevation

A hydrologically conditioned digital surface model (DEM) was derived from the NASA Shuttle Radar Topography Mission version 3.0 Global 1 arc second (SRTMGL1). Hydrological corrections ensured accurate representation of hydrological networks, with adjustments made using SAGA GIS software (Conrad et al., 2015). Basin delineation and analysis were conducted using QGIS and Tanalys software (Schulla, 2021) to extract essential topographic information for hydrological modeling.

2.2.3 Soil type

Soil data were sourced from the SIIGSOL 100-meter resolution database, which provides detailed descriptions of sand, clay, and silt proportions within the soil profile (Ministère des Ressources Naturelles et des Forêts, 2022; Sylvain et al., 2021). These proportions were converted to soil texture classes based on the USDA classification system (Soil Survey Division Staff, 2017). Soil hydraulic properties were imputed from established relationships between soil texture classes and hydraulic parameters. Elevation data were used to account for soil depth variability, by classifying raster cells into deep, normal, and shallow categories based on their relative elevation.

2.2.4 Land use

Land use data were obtained from the 2015 North American Land Change Monitoring System (NALCMS) 30-meter resolution dataset. These data were resampled using the nearest neighbor method to create land use maps, significantly impacting hydrological parameters such as root distribution, vegetation cover fraction (VCF), roughness length (Z0), and albedo. These parameters influence processes like evapotranspiration, runoff, and infiltration (2015 Land Cover of North America at 30 meters, 2023; Latifovic et al., 2012).

https://doi.org/10.5194/egusphere-2025-4450
Preprint. Discussion started: 18 September 2025

2.2.5 Climate model data

Projected daily temperature and precipitation data were sourced from the Coupled Model Intercomparison Project Phase 6 (CMIP6) (O'Neill et al., 2016) for both the reference period (1981-2010) and future period (2070-2099). These datasets were accessed and processed through the PAVICS-Hydro platform (Arsenault et al., 2023). The Shared Socioeconomic Pathway 5-8.5 (SSP5-8.5) scenario, which projects very high greenhouse gas emissions, was used to simulate future conditions (Calvin et al., 2023). To address uncertainties related to climate model selection, an ensemble of 18 climate models was employed as it was previously shown that, to ensure robustness, using multiple climate models is required (Arsenault et al., 2020; Lucas-Picher et al., 2021; Minville et al., 2008; Tarek et al., 2021). This ensemble approach ensures a more robust representation of potential climate outcomes by capturing a range of possible future scenarios. Table A1 provides a list of GCMs along with their respective institutions and horizontal resolutions.

To assess the reliability of the selected climate models, their ability to reproduce historical precipitation and temperature patterns was evaluated over the reference period (1981–2010). Tables A2 and A3 respectively present the monthly precipitation bias (%) and temperature bias (°C) for each model compared to ERA5, averaged across the 10 study catchments. These tables highlight seasonal discrepancies and allow the assessment of GCM performance. There is notable variability in precipitation biases among models. Some models, such as FGOALS-g3 and NorESM2-LM, exhibit consistently negative biases across most months (mean of bias of -16.4% for both models). In contrast, IPSL-CM6A-LR and INM-CM4-8 show persistent overestimations, with mean biases of +17.5% and +9.9%, respectively. Temperature biases also show systematic trends, with models like EC-Earth3-Veg-LR and EC-Earth3 exhibiting cold biases below -2°C, while MIROC6 and ACCESS-ESM1-5 systematically overestimate temperatures (mean of +1.8% and +1.6% respectively), particularly in summer. Despite these biases, all models were retained to maintain consistency with broader climate impact assessments, ensuring a diverse ensemble that captures a range of potential climate outcomes.

The resolution of the selected CMIP6 global climate models (GCMs) varies, with some models, such as IPSL-CM6A-LR, providing a finer resolution of 1.25° × 2.5°, while others, like CanESM5, retain a coarser resolution of 2.8° × 2.8°. Given that the hydrological model operates at a 1000-meter spatial resolution, a method was required to bridge the resolution gap between GCMs and WaSiM. To address this, WaSiM internally applies inverse distance weighting (IDW) interpolation, ensuring that the coarse-resolution GCM data is adjusted to match the finer hydrological grid. This approach ensures that all methods remain comparable by using climate models at the same spatial resolution. External statistical or dynamical downscaling methods were deliberately avoided to maintain methodological consistency between the three methods. Additionally, since this study focuses on 30-year climatological trends rather than individual events, the impact of finer-resolution climate inputs is expected to be minimal when averaged over long periods. Finally, this methodological choice streamlines the study by avoiding additional uncertainty and complexity associated with external downscaling techniques, which could introduce biases unrelated to the comparative evaluation of hydrological modeling methods.

https://doi.org/10.5194/egusphere-2025-4450
Preprint. Discussion started: 18 September 2025

2.3 Hydrological modeling

2.3.1 Hydrological model

WaSiM is a physically based, spatially distributed hydrological model designed to simulate water flow processes in catchments. It integrates a comprehensive suite of sub-models to capture key hydrological processes, including surface runoff, groundwater recharge, interflow, and baseflow, within a deterministic framework (Schulla, 2021). In this study, WaSiM was configured with a spatial resolution of 1000 meters and a temporal resolution of 24 hours. This setup allows for detailed spatial analysis while maintaining computational efficiency. The chosen spatial resolution ensures that the heterogeneity of the landscape is adequately captured, and the daily time step allows for accurate simulation of hydrological processes over time. WaSiM employs the Richards equation and the Van Genuchten parameters for simulating water flow in the unsaturated zone (van Genuchten, 1980; Richards, 1931). This equation provides a physically based representation of hydraulic head gradients and soil moisture dynamics, incorporating detailed soil physical properties. Groundwater flow is calculated conceptually within the unsaturated zone model.

2.3.2 Conventional method

The framework used to calibrate and validate the effectiveness of the conventional method rely on the split sample test (SST) approach, which is widely recognized for its effectiveness in evaluating model performance. This approach involves dividing the data into separate calibration and validation periods, allowing for an assessment of the model's ability to generalize beyond the calibration conditions. For this method, historical data from ERA5 were used for both calibration and validation. The calibration period spanned from 2000 to 2009, during which simulations were performed over a 15-year period (1995 to 2009), discarding the first 5 years to stabilize the initial conditions of the model. The validation period was set from 1990 to 1999, following the same approach of conducting simulations over a 15-year period (1985 to 1999) and discarding the initial 5 years. A set of 17 parameters (Table 2) was selected for calibration based on model documentation. Table 2 was taken from Talbot et al. (2024a).

https://doi.org/10.5194/egusphere-2025-4450
Preprint. Discussion started: 18 September 2025

Table 2. Calibration parameters for the hydrological model WaSiM.

No.	Code	Description	Sub-Model	Range
1	k_D	Storage coefficient for surface runoff (h)	Unsaturated zone	[1, 25]
2	k_H	Storage coefficient for interflow (h)	Unsaturated zone	[1, 25]
3	KB	Storage coefficient for base flow (m)	Unsaturated zone	[0.1, 8]
4	Q0	Scaling factor for base flow (mm h^{-1})	Unsaturated zone	[0.1, 5]
5	d_r	Drainage density for interflow (m^{-1})	Unsaturated zone	[1, 50]
6	QD_{Snow}	Fraction of surface runoff on snow melt	Unsaturated zone	[0.1, 1]
7	c_0	Degree-Day factor (mm $°C^{-1}$ d^{-1})	Snow	[0, 3]
8	T_0	Temperature limit for snow melt (°C)	Snow	[-4, 4]
9	$T_{R/S}$	Transition temperature snow/rain (°C)	Snow	[-4, 4]
10	C_{WH}	Water storage capacity of snow	Snow	[0.1, 0.3]
11	C_{rfr}	Coefficient for refreezing	Snow	[0.1, 1]
12	$f_{i,summer}$	Summer correction factors for PET	Evapotranspiration	[0.1, 2]
13	$f_{i,fall}$	Fall correction factors for PET	Evapotranspiration	[0.1, 2]
14	$f_{i,winter}$	Winter correction factors for PET	Evapotranspiration	[0.1, 2]
15	$f_{i,spring}$	Spring correction factors for PET	Evapotranspiration	[0.1, 2]
16	K_{rec}	Recession constant for hydraulic conductivity	Soil table	[0.1, 0.99]
17	d_z[a]	Soil layer thickness	Soil table	[0.8, 1.4]

[a] Calibration coefficient, ranging from 0.8 to 1.4, is applied to adjust the total soil depth, which is predetermined to be 8 meters for shallow, 14 meters for normal, and 20 meters for deep soil conditions.

These parameters were optimized based on a single objective function through the Dynamically Dimensioned Search (DDS) algorithm, developed by Tolson and Shoemaker (2007). This algorithm was chosen for its efficiency in handling complex optimization problems for compute-intensive hydrological models, as recommended by Arsenault *et al.* (2014).

The objective function used for calibration was the Kling Gupta-Efficiency (KGE) (Kling et al., 2012). The KGE metric provides a balanced evaluation of model performance by considering simultaneously correlation, variability, and bias in the simulated streamflow relative to observed streamflow. The KGE is computed using Eq. (1):

$$KGE = 1 - \sqrt{(r-1)^2 + \left(\frac{\sigma_{sim}/\mu_{sim}}{\sigma_{obs}/\mu_{obs}} - 1\right)^2 + \left(\frac{\mu_{sim}}{\mu_{obs}} - 1\right)^2}, \quad (1)$$

where r is the Pearson correlation coefficient between simulated and observed streamflow, σ_{sim} is the standard deviation of simulated streamflow, σ_{obs} is the standard deviation of observed streamflow, μ_{sim} is the mean of the simulated streamflow, and μ_{obs} is the mean of the observed streamflow. A KGE value of 1 indicates a perfect match between the simulated and observed streamflow, reflecting ideal performance across all three components: correlation, variance, and bias.

https://doi.org/10.5194/egusphere-2025-4450
Preprint. Discussion started: 18 September 2025

For the conventional method, the Multivariate Bias Correction algorithm (MBCn) developed by Cannon (2018) was used to correct biases in the climate model simulations. This method corrects biases in meteorological data while accounting for spatiotemporal interdependencies between variables and preserving changes in quantiles between the reference (1981-2010) and future (2070-2099) periods. The bias correction was applied to daily total precipitation and daily mean temperature using ERA5 data as the reference over the period 1981-2010 and was used to correct the climate models data for both the reference (1981-2010) and future periods (2070-2099). Climate change studies were subsequently conducted using bias-corrected climate model data. Hydrological simulations were carried out for each climate model over both the reference and future periods, using a hydrological model calibrated with raw data for each catchment.

2.3.3 Fully asynchronous method

The primary objective of the fully asynchronous method is to conduct climate change studies without relying on observed meteorological data (Ricard et al., 2019, 2020, 2023; Valencia Giraldo et al., 2023) and eliminate the need for bias-correction of climate variables. Instead, the calibration is performed using raw climate model data and observed streamflow, integrating the bias-correction in the calibration step. A significant challenge in this approach is the lack of synchronization between the timings of observed streamflows and those of raw climate model outputs (Ricard et al., 2019), as climate models are not temporally aligned with actual past events. This requires a departure from the conventional calibration framework, which aims to optimize the timing and amplitude of streamflow. To overcome this obstacle, the objective function optimizes the distribution of observed streamflow over an extended period rather than individual streamflow observations. This approach ensures that the hydrological model effectively preserves the streamflow distribution, rather than capturing day-to-day natural variability.

Given the calibration objectives of the fully asynchronous method, the observed streamflow data from 1984 to 2009 was sorted and used to establish a reference distribution of streamflow. This sorted distribution provided a consistent target for both the calibration and validation of the hydrological model. In the context of the fully asynchronous method, where direct temporal alignment between climate model outputs and observed streamflow is not maintained, relying on the same observed distribution for both calibration and validation ensures that the model is evaluated against a stable and representative reference. Therefore, a 25-year period (1984–2009) of hydrometric station data was selected for calibration and validation to capture a wide range of hydrological conditions. This duration helps reduce the impact of short-term climate variability and minimizes biases associated with shorter time frames. A key hypothesis underlying this approach is the assumption of stationarity, that the hydrological model, with fixed parameters optimized during calibration, will continue to produce reasonable streamflow simulations under future climate conditions. This assumes that despite changing climatic conditions, the model will adequately respond to future scenarios as it did to past conditions. However, if future climate changes introduce conditions outside the model's calibrated range, such as new snow patterns or shifts in seasonal dynamics, the model's performance could be compromised. It is important to recall that the conventional method also relies on two stationarity assumptions, namely that

https://doi.org/10.5194/egusphere-2025-4450
Preprint. Discussion started: 18 September 2025

the calibrated parameters of the hydrological model remain valid under future conditions and that the bias correction applied to the climate data continues to hold under a changing climate.

The calibration and validation periods are separated based on the total yearly precipitation from October to September. This separation ensures an equal distribution of wet and dry years between both periods. Simulations were performed for the years 1984 to 2011, with the first two years discarded to allow for initial model stabilization. Out of the 26 years of simulations, 13 years were used for calibration, selected based on total yearly precipitation, while all 26 years were utilized for model validation.

To address biases in simulated streamflow resulting from biases in raw climate data, the simulated streamflow was adjusted by multiplying it by a factor equal to the ratio of the mean observed streamflow Q_{obs} to the mean simulated streamflow Q_{sim}. This adjustment was applied only during the calibration process and not during the reference or future periods simulations. It ensures that the mean simulated streamflow matches the mean observed streamflow, effectively removing bias and allowing the optimization algorithm to focus on matching the shape of the streamflow distribution rather than its absolute magnitude. This means the simulated absolute streamflow values cannot be directly compared with observations, but changes between the reference and future period can be analyzed.

An essential aspect of the fully asynchronous method is its focus on calibrating the model based on the distribution of streamflow rather than its temporal sequence. Given this objective, Root Mean Square Error (RMSE) was selected as the calibration metric due to its ability to emphasize overall distributional accuracy while penalizing large deviations between simulated and observed streamflow values. RMSE effectively captures the spread and magnitude of streamflow across different flow conditions, ensuring that extreme and median flows are well represented. Unlike correlation-based metrics, which prioritize timing accuracy, RMSE remains robust when applied to sorted streamflow values, aligning well with the fully asynchronous method's goal of preserving statistical consistency rather than event-specific timing. Additionally, RMSE provides a straightforward optimization framework, allowing for efficient parameter tuning without introducing unnecessary complexity into the calibration process. The RMSE was computed on the flow duration curves of the simulated and observed flows using equation 2:

$$RMSE = \sqrt{\frac{1}{n}\sum_{i=1}^{n}((sort(Q_{sim})_i - (sort(Q_{obs})_i)^2} \quad , \tag{2}$$

where Q_{sim} represents the simulated streamflow (mm), Q_{obs} represents the observed streamflow (mm), sort() is the function that sorts the sequence in descending order, and n is the number of simulated streamflow values.

Each climate model was calibrated for each catchment, resulting in a total of 180 calibration parameter sets (18 climate models x 10 catchments). In contrast, the conventional method involves 10 calibration parameter sets (one per catchment) which is then applied to all climate models and their bias-corrected outputs. Consequently, the fully asynchronous method is considerably more computationally intensive than the conventional method in terms of parameter calibration.

The calibration framework for the fully asynchronous method is similar to that of the conventional method (Section 2.3.2). It involves 1000 evaluations, uses the same 17 calibration parameters (Table 2), and employs the DDS optimization algorithm.

https://doi.org/10.5194/egusphere-2025-4450
Preprint. Discussion started: 18 September 2025

For the fully asynchronous method, climate change simulations were conducted using the calibrated model for each catchment and each projected climate model, but without relying on historical event timing. Raw projected climate data were utilized to perform simulations over both the reference and future periods. Figure 2 presents a workflow diagram of the fully asynchronous method, adapted from Ricard et al. (2023).

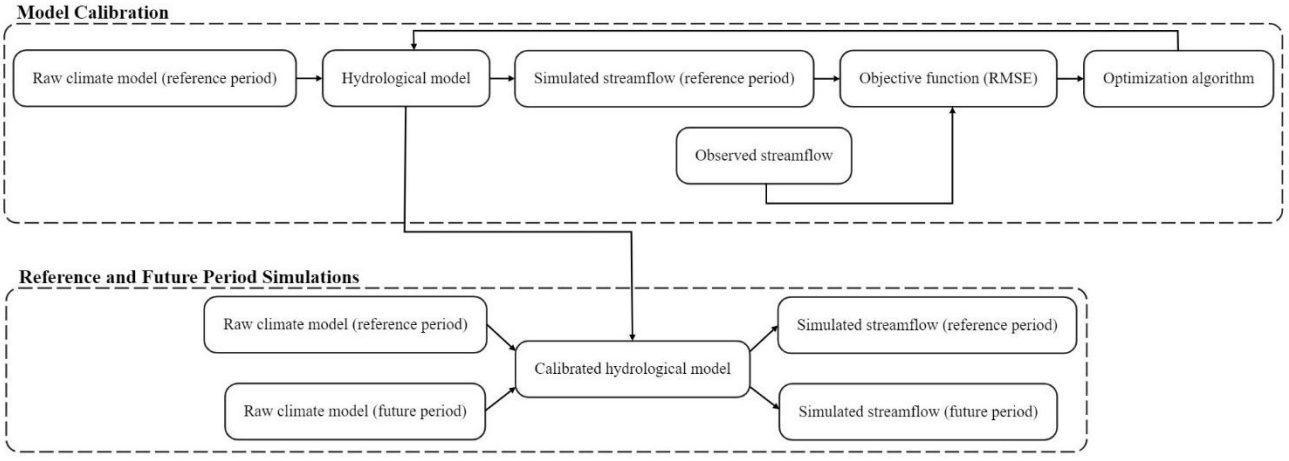

Figure 2. Workflow diagram of the fully asynchronous method.

2.3.4 Semi-asynchronous method

In addition to the conventional and fully asynchronous approaches, a semi-asynchronous method was developed and tested in this study. This method follows the same overall framework as the fully asynchronous approach but introduces an element to account for temporal dependencies in the objective function used during calibration. Specifically, rather than computing the RMSE over the entire streamflow distribution, the RMSE is calculated on the sorted streamflow separately for each calendar month, thereby capturing seasonal variations more explicitly. The overall objective function for the semi-asynchronous method is defined as a weighted average of monthly RMSE values, as shown in Equation (3):

$$RMSE_{sa} = \frac{1}{12}\sum_{m=1}^{12}(\alpha_m * RMSE_m) \quad (3)$$

In this equation, $RMSE_{sa}$ is the semi-asynchronous RMSE used as the objective function, and $RMSE_m$ refers to the RMSE between the sorted simulated and observed streamflow values for calendar month m, from January to December, as detailed in equation 2. α_m is equal to 1 and represents a weighting coefficient that determines the importance of that month in the overall calibration. By grouping streamflow values by month and comparing the corresponding sorted distributions, the semi-asynchronous method introduces partial synchronicity into the calibration process. The proposed design preserves the underlying hypothesis of the fully asynchronous method in reproducing streamflow distributions, while also incorporating seasonal characteristics of key hydrological events. This is achieved through a mechanism that introduce a monthly structure,

https://doi.org/10.5194/egusphere-2025-4450
Preprint. Discussion started: 18 September 2025

aiming to better capture intra-annual dynamics such as snowmelt, runoff generation, and other seasonal processes without relying on full temporal alignment.

2.4 Comparative analysis

The analysis in this study is designed to compare the performance of the conventional, fully asynchronous, and semi-asynchronous methods in simulating hydrological processes under both current and future climate conditions. To ensure a fair and unbiased comparison, all three methods employed the same WaSiM configuration, including identical calibration parameters, the number of evaluations, and the optimization algorithm. This was performed to ensure minimal calibration bias and to isolate the differences attributable solely to the methodological framework of each approach.

The first step in the analysis involves assessing the calibration and validation performance of each method. Streamflow simulations were evaluated using the Kling-Gupta Efficiency (KGE) for the conventional method and the root mean square error (RMSE) between sorted simulated and observed streamflow values for both the fully asynchronous and semi-asynchronous methods. These metrics were selected to highlight each method's respective strengths, with KGE capturing overall model performance and RMSE emphasizing accuracy in reproducing the streamflow distribution.

Beyond streamflow, the relationships between various hydroclimatic variables, such as groundwater recharge, surface runoff, soil moisture, and snow water equivalent (SWE) were also examined. By comparing the simulated values from all three methods, the analysis seeks to understand how well each method captures the interactions between these variables. This serves to evaluate the internal consistency of the models and assess their ability to realistically simulate the physical processes within the catchments.

The analysis extends to a comparison of the projected changes in hydroclimatic variables between the reference period (1981–2010) and the future period (2070–2099). The magnitude and direction of these changes are assessed to determine how each method projects the impact of climate change on the catchment's hydrological processes. This includes examining variables such as changes in snowmelt dynamics and the consequent effects on streamflow, surface runoff and groundwater recharge. A detailed spatial analysis is also conducted to evaluate the distribution of such key variables across the catchments. The comparative analysis employs several criteria to determine which method is most effective. These include the accuracy of streamflow simulation (both in terms of overall distribution and event timing), the internal consistency of hydroclimatic variable relationships and the realism of spatial distributions and projected changes under future climate scenarios.

3 Results

3.1 Streamflow representation

For the conventional method, streamflow representation performance was assessed using the KGE metric for each catchment during both the calibration and validation periods.

https://doi.org/10.5194/egusphere-2025-4450
Preprint. Discussion started: 18 September 2025

During calibration, the conventional method achieves KGE values ranging from 0.817 to 0.906, with a mean of 0.863. Similarly, for the validation period, the KGE values ranged from 0.778 to 0.906, with a mean of 0.842. These results indicate that the conventional method maintains a consistent performance in simulating streamflow across different catchments. Detailed KGE results for each catchment are provided in the Appendix B (Table B1).

For the fully asynchronous and semi-asynchronous methods, streamflow representation performance was evaluated using the RMSE calculated on sorted daily streamflow values. For the fully asynchronous method, the mean RMSE during calibration was 0.121 mm d^{-1}, with an inter-model standard deviation of 0.031 mm d^{-1}. In the validation period, the mean RMSE increased slightly to 0.179 mm d^{-1}, with a standard deviation of 0.057 mm d^{-1}. The semi-asynchronous method showed higher RMSE values overall, with a mean of 0.282 during calibration and 0.285 during validation. To enable direct comparison, the sorted RMSE was also computed for the conventional method, yielding values of 0.497 for calibration and 0.518 for validation. These results indicate that, in terms of streamflow distribution alone, the fully-asynchronous method performed best, followed by the semi-asynchronous method, and finally the conventional method. This ranking highlights the strengths of the distribution-focused calibration used in the fully asynchronous approaches. Detailed RMSE results for all methods and catchments are provided in Appendix B (Table B2).

Figure 3 presents hydrographs of streamflow for all three methods during the reference period across the ten catchments, along with observed streamflow for the same period. The fully asynchronous method shows greater variability between climate models, especially in the timing of peak flows, which often fails to align with the observed data, as expected. This variability suggests that the timing of streamflow events in the fully asynchronous method is highly sensitive to the specific climate model employed. For instance, in the Matane catchment, the observed and conventional method peak flow occurs at the beginning of May, while the fully asynchronous method shows a broader range of peak flow timings, extending from early May to late June. This discrepancy might be attributed to challenges in accurately simulating snowmelt processes with the fully asynchronous method, which are crucial for generating high flows in snowy catchment. Furthermore, in the same catchment, the fully asynchronous method overestimates summer flows compared to the observed data, indicating potential difficulties in capturing the seasonal dynamics of low-flow periods. Conversely, the semi-asynchronous and conventional methods both succeed in capturing the seasonal timing and magnitude of streamflow events, closely aligning with the observed hydrographs. The conventional method offers the most consistent performance across climate models, with peak flows and low-flow periods well synchronized with observations on the reference period. The semi-asynchronous method also accurately reproduces the overall seasonal streamflow pattern, including the timing of snowmelt-driven peak flows. Although it introduces slightly more inter-model variability than the conventional method, this variability remains lower than that observed in the fully-asynchronous method.

https://doi.org/10.5194/egusphere-2025-4450
Preprint. Discussion started: 18 September 2025

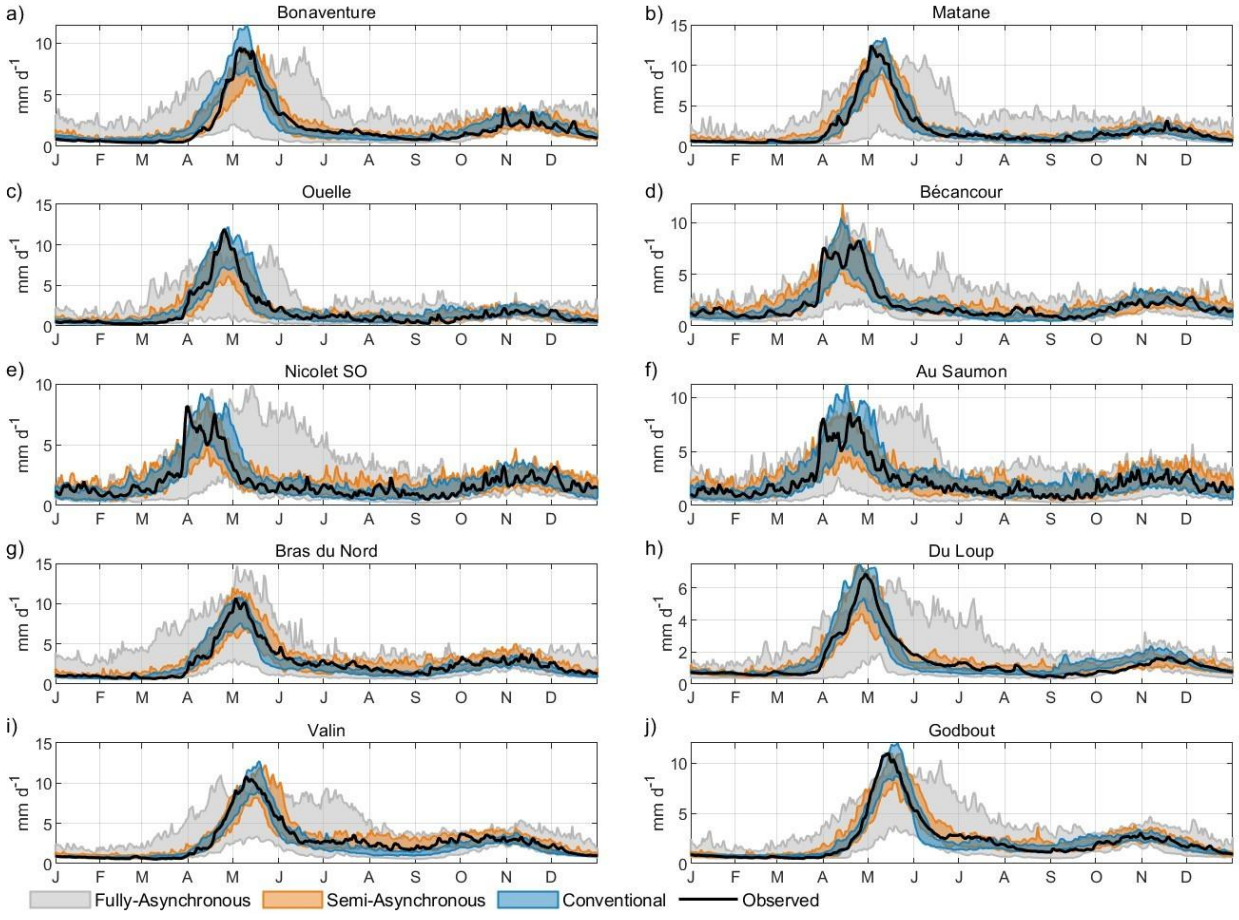

375 **Figure 3. Seasonal streamflow comparison between the fully asynchronous, semi-asynchronous and conventional methods and observed data across ten catchments during the reference period (1981–2010). The panels (a-j) represent the catchments of Bonaventure, Matane, Ouelle, Bécancour, Nicolet SO, Au Saumon, Bras du Nord, Du Loup, Valin, and Godbout, respectively.**

Figure 4 presents the relationship between sorted streamflow values and percentage bias for simulated versus observed streamflow using the three methods during the reference period (1981 to 2010) for the Matane catchment. The fully
380 asynchronous method shows the lowest percentage bias across a wide range of streamflow conditions, particularly at the extremes, reflecting its strong ability to capture the full distribution of flows. This performance stems from its calibration strategy, which explicitly targets the statistical distribution of streamflow rather than the timing of individual events.

The semi-asynchronous method offers intermediate performance between the fully asynchronous and conventional methods. It more accurately represents the streamflow distribution than the conventional approach, particularly for high and low flows,
385 but shows slightly greater bias than the fully asynchronous method. This outcome suggests that the incorporation of monthly structure into the calibration helps preserve distributional accuracy while also improving the temporal realism of seasonal flow patterns. In contrast, the conventional method shows broader dispersion in bias and tends to underperform in reproducing extreme events, especially at high flows. While Figure 4 focuses on the Matane catchment, similar patterns are observed across

https://doi.org/10.5194/egusphere-2025-4450
Preprint. Discussion started: 18 September 2025

the other study catchments (Figures C1 to C9), reinforcing the generalizability of these results. Together, these findings highlight a key trade-off in hydrological modeling under climate change, where the fully asynchronous method excels in preserving streamflow distribution and extremes, the conventional method performs best in capturing temporal accuracy, and the semi-asynchronous method offers a promising compromise by balancing both aspects.

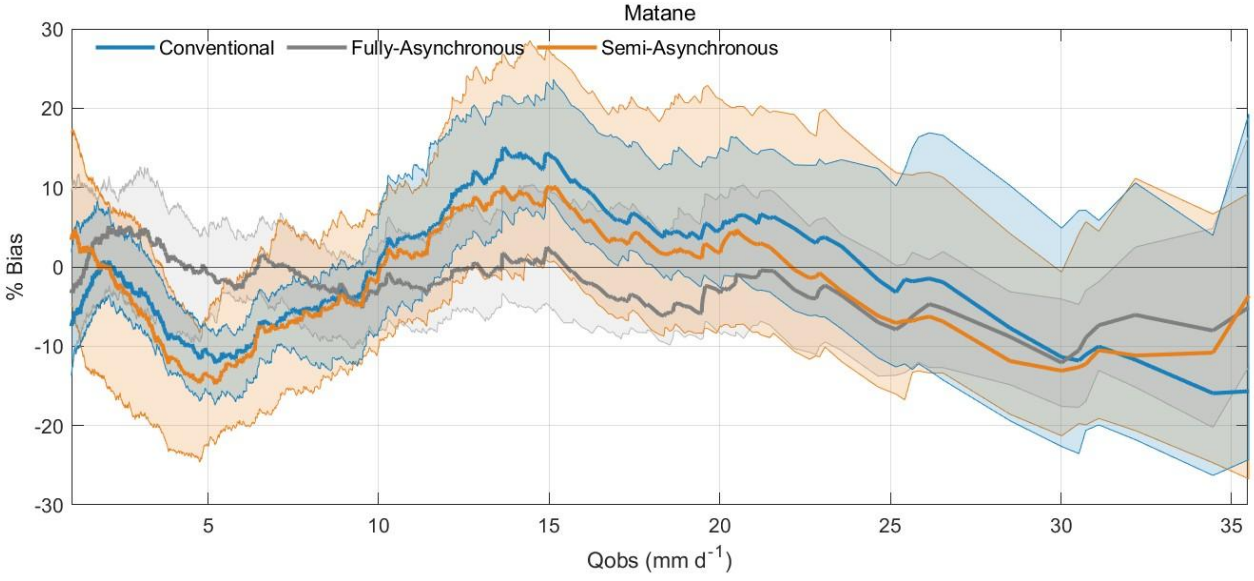

Figure 4. Performance comparison between the conventional, fully asynchronous and semi-asynchronous methods for the Matane catchment during the reference period (1981–2010). The figure shows the percentage bias between observed and simulated streamflows, with the x-axis representing the observed daily streamflow and the y-axis displaying the percentage bias relative to the observed values. The shaded regions illustrate the variability among climate models around the mean bias for each method (solid lines).

Figure 5 presents a comparative analysis of streamflow quantiles simulated by the three methods across the reference period (1981 to 2010) and the future period (2070 to 2099) for all ten catchments. When comparing the reference period simulations to observed streamflow, both the fully asynchronous and semi-asynchronous methods demonstrate closer alignment with the observed distribution, particularly for high flows (Q95). This confirms their ability to better capture streamflow extremes. Specifically, the absolute mean bias for Q95 is 2.7 % for the fully asynchronous method and 3.0 % for the semi-asynchronous method, compared to 5.2 % for the conventional method (Table D1). However, this improved accuracy comes with greater inter-model variability. For Q95 in the reference period, the standard deviation across climate models increases from 3.4 % with the conventional method to 4.8 % with the semi-asynchronous method and 6.2 % with the fully asynchronous method.

In terms of future projections, all methods show a decrease in Q95 across most catchments. The fully asynchronous method estimates a smaller reduction in Q95 at 8.4%, while the semi-asynchronous and conventional methods project similar declines of 12.5% and 13.0%, respectively (Table D1). Despite the more moderate change, the semi-asynchronous method shows the highest inter-model variability, with a standard deviation of 17.1%, while the fully asynchronous and conventional methods display similar and lower variability, at 10.0% and 9.9%, respectively.

https://doi.org/10.5194/egusphere-2025-4450
Preprint. Discussion started: 18 September 2025

For median flows (Q50), the results are more varied. During the reference period, the semi-asynchronous method achieves the lowest absolute mean bias at 2.7 %, followed by the fully asynchronous method at 5.8 %, and the conventional method at 11.3 % (Table D2). Under future conditions, all three methods project an increase in Q50, with the semi-asynchronous method projecting the largest rise at 27.6 %, followed by the conventional method at 18.0 % and the fully asynchronous method at 14.4 %. The semi-asynchronous method also displays the highest inter-model spread, with a standard deviation of 29.2 %, compared to 18.4 % for the conventional method and 17.8 % for the fully asynchronous method.

Low flows (Q5) reveal the largest discrepancies among methods. In the reference period, the fully asynchronous method shows the lowest absolute mean bias at 48.6 %, followed by the conventional method at 62.8 %, and the semi-asynchronous method at 95.4 % (Table D3). These results highlight the difficulty of all methods to accurately capture low-flow conditions. For future projections, Q5 increases by 21.9 % for the conventional method, 15,3% for semi-asynchronous and 13.8 % for the fully asynchronous method. Once again, the fully asynchronous and semi-asynchronous methods display higher variability, with standard deviations of 25.5 % and 25.3 % respectively, compared to 10.4 % for the conventional method.

Overall, the quantile-based analysis highlights the strength of the fully asynchronous and semi-asynchronous methods in capturing flow distributions and extremes, while also emphasizing their increased sensitivity to climate model variability. Detailed results across all ten catchments are provided in Tables D1 to D3.

https://doi.org/10.5194/egusphere-2025-4450
Preprint. Discussion started: 18 September 2025

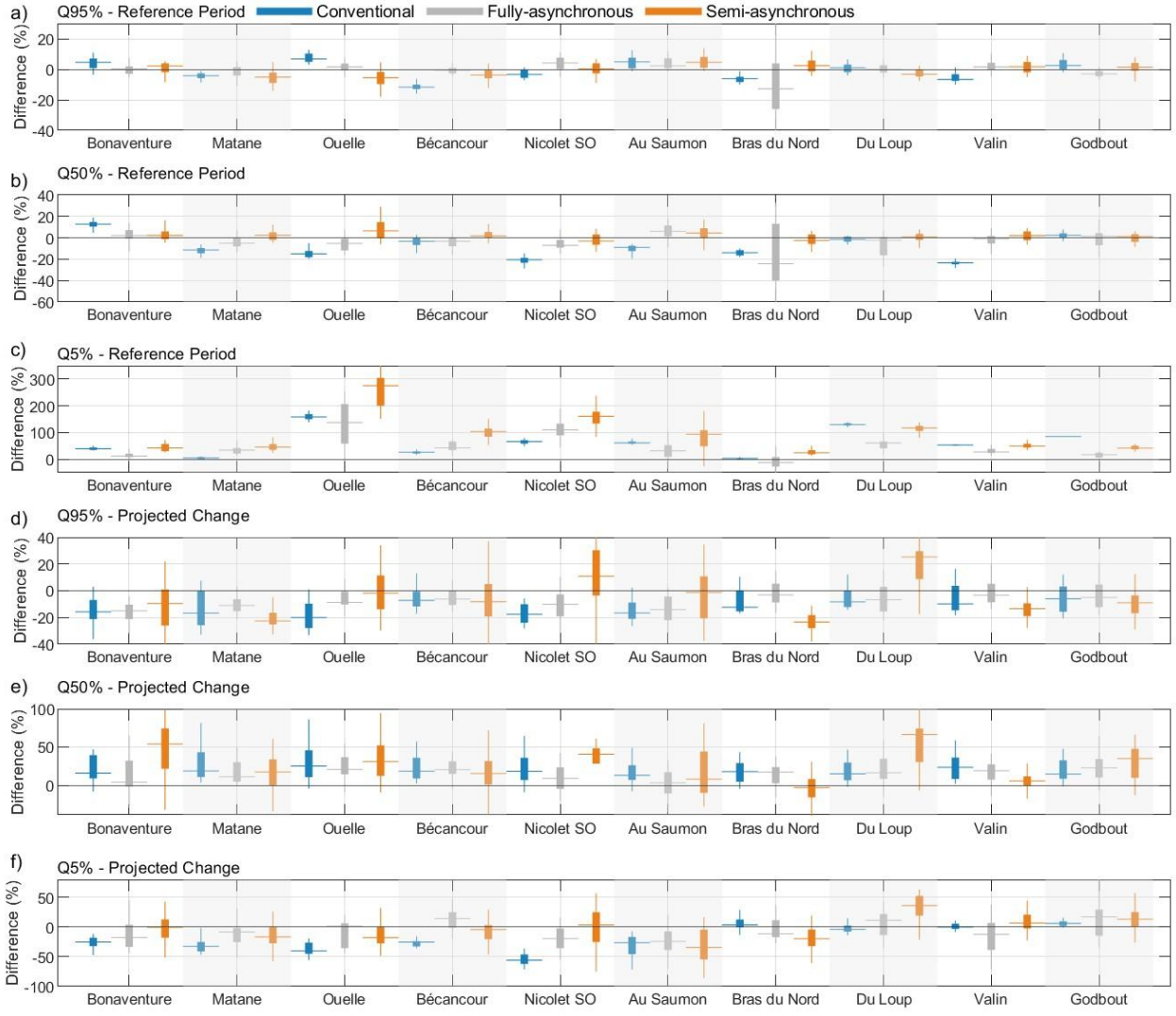

Figure 5. Comparison of streamflow distributions for the reference period (1981–2010) and projected changes in the future period (2070–2099) across 10 catchments. The plots show the percentage differences in streamflow quantiles between simulated and observed values during the reference period, and the projected changes represent the percentage differences between future and reference simulations for each method. Boxes indicate the interquartile range (25th to 75th percentiles), and central lines represent the median.

3.2 Hydroclimatic variables

In addition to streamflow, a key objective of this study is to evaluate how well the conventional, fully asynchronous, and semi-asynchronous methods simulate a broader range of hydroclimatic variables. This allows for a more comprehensive comparison of the methods' ability to reproduce the underlying hydrological processes that govern catchment behavior under current and future climate conditions.

https://doi.org/10.5194/egusphere-2025-4450
Preprint. Discussion started: 18 September 2025

To explore these dynamics in greater detail, the Matane catchment was selected as a representative case study. Covering an area of 1650 km², Matane exhibited strong calibration and validation performance across all three methods and reflects the typical hydroclimatic and physiographic conditions found across the study region. This focused analysis enables a deeper examination of how each method influences key components of the water balance, including snowmelt, surface runoff, evapotranspiration, groundwater recharge, and soil moisture.

Average monthly temperature and precipitation for the reference period (1981-2010) and the future period (2070-2099) before and after bias-correction using MBCn for the Matane catchment and the climate model ACCESS-ESM1-5 is provided as an example (Fig. 6).

In the reference period, a noticeable gap exists between the ERA5 data and the raw climate model data, with the raw climate data showing higher temperatures and increased precipitation for all months except October. The effectiveness of the bias correction is evident, as the bias-corrected climate data closely aligns with the ERA5 data, significantly reducing discrepancies in temperature and precipitation. The same bias trend is observed in the future period, where raw climate model data predicts higher temperatures and increased precipitation compared to the bias-corrected data.

Furthermore, Fig. 6 highlights the anticipated changes in precipitation and temperature between the reference and future periods. Temperatures are expected to increase significantly, with projected increases around 6 degrees Celsius across the study area. These projections are in line with the IPCC's forecasts based on SSP5-8.5, and suggest that northern latitudes will experience faster warming compared to the global average (Estrada et al., 2021). Projections consistently show an annual increase in precipitation ranging from 15 to 20%, with the most significant increases occurring between November and April, as well as in July. The anticipated increases in temperature and changes in precipitation patterns have profound implications for hydrological processes and water resource management.

https://doi.org/10.5194/egusphere-2025-4450
Preprint. Discussion started: 18 September 2025

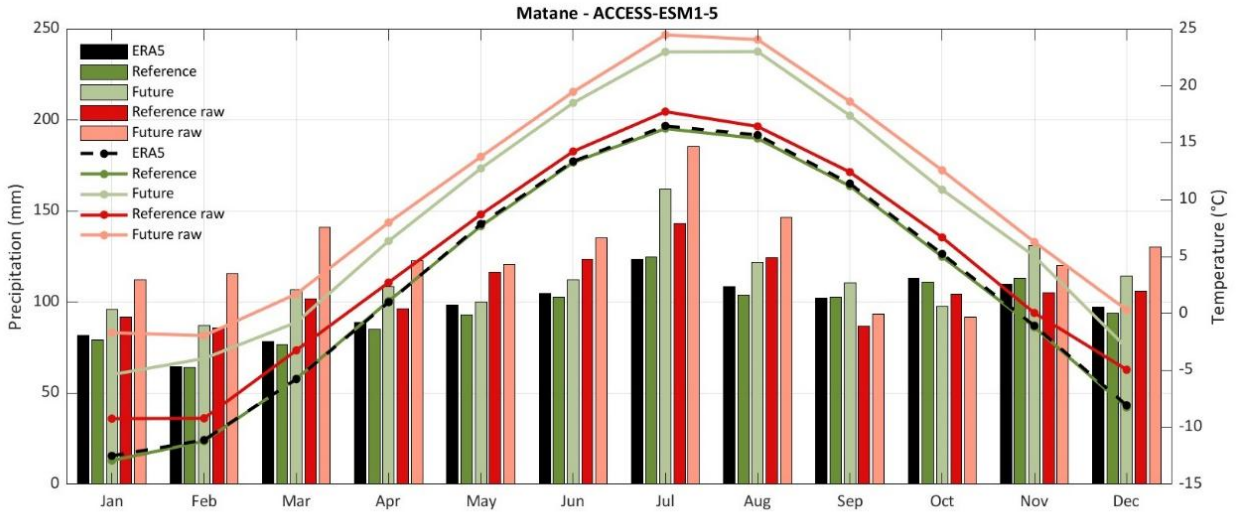

460 **Figure 6. Comparison of average monthly precipitation and temperature for the Matane catchment. This figure displays the average monthly temperature and precipitation for the Matane catchment during the reference period (1981-2010) and the future period (2070-2099) under the Shared Socioeconomic Pathway 5-8.5 (SSP585) scenario.**

Table 3 presents the annual averages of key hydroclimatic variables for both the reference period (1981 to 2010) and the future period (2070 to 2099). Results are provided for the conventional, fully asynchronous, and semi-asynchronous methods, along
465 with the relative change between periods for each variable and method. All three methods, project similar directional changes under future climate conditions. Precipitation and ETa are projected to increase, while snowfall and SWE decline significantly. These changes are consistent with the expected response to warming, where higher temperatures reduce snow accumulation and increase atmospheric demand for water. For instance, SWE decreases by more than 50% across all methods, while ETa increases by approximately 31%-32%.

470 Despite these common trends, notable differences are observed in the magnitude and representation of certain variables. Surface runoff stands out as the most divergent. The fully asynchronous method simulates more than twice the amount of surface runoff compared to the conventional method during the reference period, a pattern that persists in future projections. This discrepancy could be due to the fully asynchronous method's misrepresentation of the timing of snowmelt, leading to amplified runoff responses. The semi-asynchronous method moderates this behavior, producing runoff values that are closer
475 to those of the conventional method, although still elevated. This suggests that the inclusion of monthly calibration in the semi-asynchronous method helps correct some of the temporal misalignments present in the fully asynchronous approach.

Groundwater recharge also shows significant differences. The fully asynchronous method simulates a relatively large increase of 19% between the reference and future periods, compared to only 4% with the conventional method. The semi-asynchronous method again produces an intermediate value of 9%. Similar patterns are observed in other components of the water balance.

https://doi.org/10.5194/egusphere-2025-4450
Preprint. Discussion started: 18 September 2025

Streamflow values appear relatively consistent across methods and periods, with projected changes ranging from 1 to 2%. Soil moisture shows smaller differences between methods, although the semi-asynchronous method again occupies an intermediate position.

Table 3. Comparison of hydroclimatic variables between the reference (1981–2010) and future (2070–2099) periods for the conventional, fully asynchronous and semi-asynchronous methods across 10 catchments and 18 climate models.

Hydroclimatic Variables	Unit	Conventional			Fully-asynchronous			Semi-asynchronous		
		Reference (1981-2010)	Future (2070-2099)	Relative Change	Reference (1981-2010)	Future (2070-2099)	Relative Change	Reference (1981-2010)	Future (2070-2099)	Relative Change
Precipitation	mm yr^{-1}	1276	1463	15%	1328	1507	13%	1328	1507	13%
Snowfall	mm yr^{-1}	409	273	-33%	362	214	-41%	392	243	-38%
Streamflow	mm yr^{-1}	730	744	2%	771	778	1%	792	799	1%
Surface Runoff	mm yr^{-1}	109	77	-29%	256	199	-22%	175	128	-26%
Interflow	mm yr^{-1}	482	530	10%	400	460	15%	445	497	12%
ETa	mm yr^{-1}	554	727	31%	561	733	31%	541	714	32%
Baseflow	mm yr^{-1}	140	137	-2%	113	117	3%	172	173	1%
Groundwater Recharge	mm yr^{-1}	133	139	4%	118	141	19%	162	176	9%
SWE	mm	281	131	-53%	252	106	-58%	276	108	-61%
Soil Moisture	-	0.188	0.180	-5%	0.203	0.200	-2%	0.193	0.188	-3%

Figure 7 illustrates the annual cycle of key hydroclimatic variables in the Matane catchment for both the reference period (1981–2010) and the future period (2070–2099). The left column shows simulations during the reference period, the middle column corresponds to the future period, and the right column displays the absolute change between the two. Shaded areas represent the spread across the 18 climate models. Equivalent figures for the other catchments are available in Appendix F.

Focusing first on the reference period, the fully asynchronous method stands out for its high inter-model variability, particularly in snow dynamics. The timing of maximum SWE varies widely, with some models showing snowmelt beginning as early as late April and extending into July. This prolonged melt period is unrealistic for the Matane region, where snow typically disappears by the beginning of June. Such an extended melt season in a 30-year average suggests a clear limitation of the fully asynchronous method in accurately capturing seasonal snow processes.

This misrepresentation has cascading effects on other components of the hydrological cycle. Surface runoff, actual evapotranspiration, and groundwater recharge simulated by the fully asynchronous method also exhibit elevated variability and inconsistencies. In its effort to reproduce the observed streamflow distribution without aligning events temporally, the fully asynchronous method tends to distort internal processes, leading to simulations that lack physical plausibility and seasonal coherence. These shortcomings undermine confidence in the method's use for climate change impact assessments in snow-dominated regions.

In contrast, the semi-asynchronous method substantially reduces the inter-model variability observed in the fully asynchronous approach, particularly for streamflow and SWE. Snowmelt timing is notably improved, aligning more closely with expectations

https://doi.org/10.5194/egusphere-2025-4450
Preprint. Discussion started: 18 September 2025

for the Matane catchment. This correction enhances the seasonal dynamics of streamflow and groundwater recharge, making the simulations more physically realistic. However, some issues remain. The semi-asynchronous method still shows greater variability in ETa compared to the conventional method. This is likely due to the use of raw, uncorrected climate model inputs in both asynchronous approaches, whereas the conventional method benefits from bias-corrected meteorological data. The model compensates for climate model biases by adjusting evapotranspiration to close the water balance, which can lead to unrealistic variability for this variable. The conventional method produces well-defined spring peaks in streamflow and interflow with lower inter-model variability. Its outputs are more consistent across models, enhancing confidence in its projections.

For the future period, the semi-asynchronous and conventional methods produce similar results for SWE, streamflow, and groundwater recharge, though the semi-asynchronous method shows greater variability in surface runoff and ETa. The fully asynchronous method continues to exhibit the highest variability across climate models, further diminishing confidence in its outputs.

Regarding the absolute changes between the reference and future periods, the semi-asynchronous and conventional methods yield comparable trends for SWE and groundwater recharge. The semi-asynchronous method produces slightly smaller variations in absolute change for streamflow and interflow, but slightly larger variations for surface runoff. Due to the high variability observed in both the reference and future periods, the fully asynchronous method offers limited reliability in its estimates of absolute change. Taken together, these results confirm that while the semi-asynchronous method offers clear improvements over the fully asynchronous approach, particularly in representing snowmelt and reducing variability, it does not yet match the stability or reliability of the conventional method for detailed climate impact assessments.

https://doi.org/10.5194/egusphere-2025-4450
Preprint. Discussion started: 18 September 2025

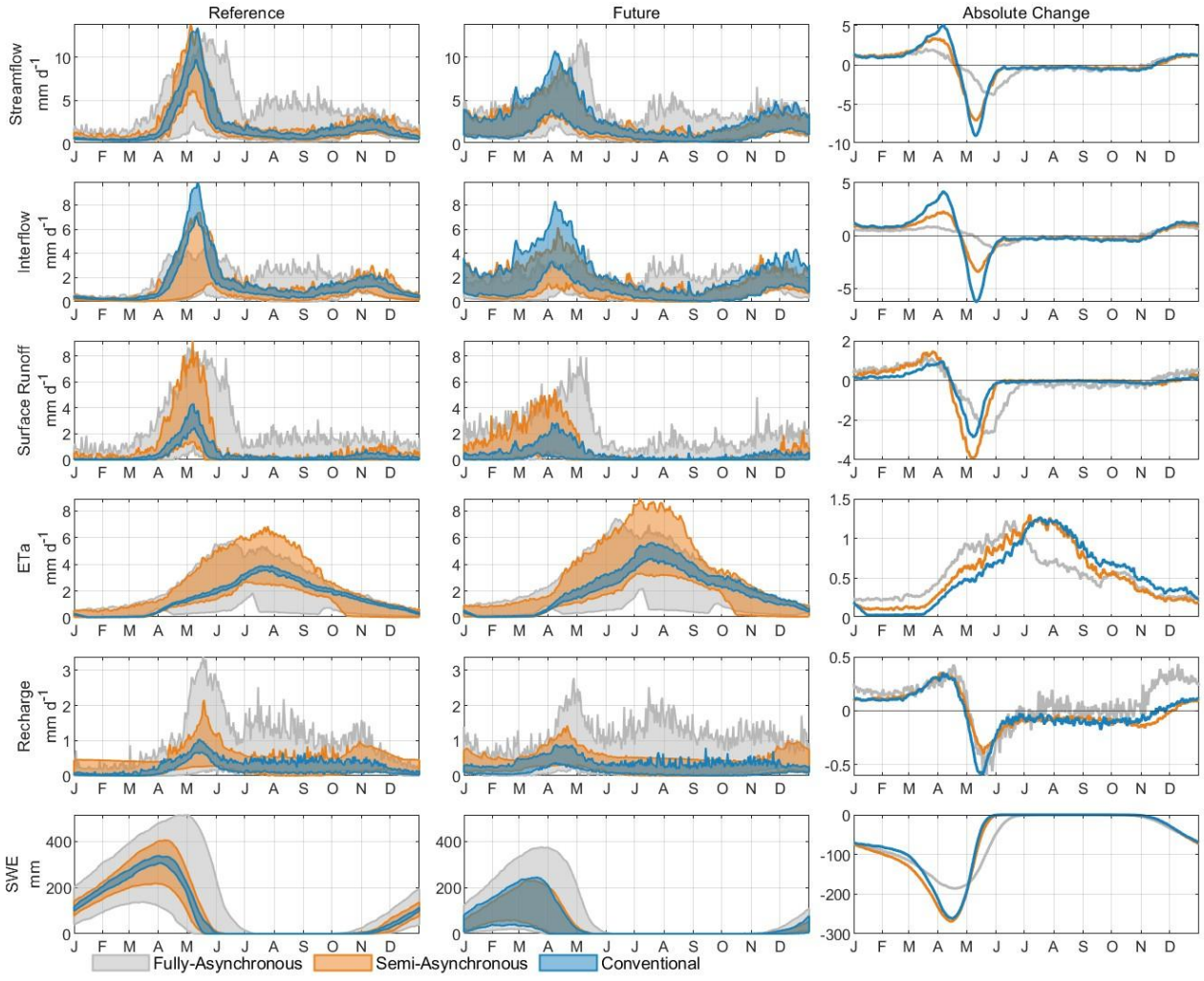

Figure 7. Seasonal distribution of key hydroclimatic variables for the reference period (1981–2010), future period (2070–2099), and their average absolute changes across the Matane catchment.

Figure 8 illustrates the spatial distribution of annual groundwater recharge rates in the Matane catchment for both the reference (1981–2010) and future (2070–2099) periods, based on simulations from the conventional, fully asynchronous, and semi-asynchronous methods. All methods exhibit similar spatial patterns, with higher elevations showing reduced recharge rates and lower elevations demonstrating higher recharge rates. An elevation map of the Matane catchment is provided in the Appendix E (Fig. E1). The semi-asynchronous method, however, predicts a generally higher magnitude of recharge across the catchment.

When examining the absolute difference between the future and reference periods, all methods project a similar spatial pattern of changes in groundwater recharge, with a noticeable decrease in recharge at lower elevations. However, the fully

https://doi.org/10.5194/egusphere-2025-4450
Preprint. Discussion started: 18 September 2025

asynchronous and semi-asynchronous methods project smaller increases in recharge in certain higher elevation areas, while the conventional method predicts a much more pronounced reduction, 3 to 4 times greater, at lower elevations.

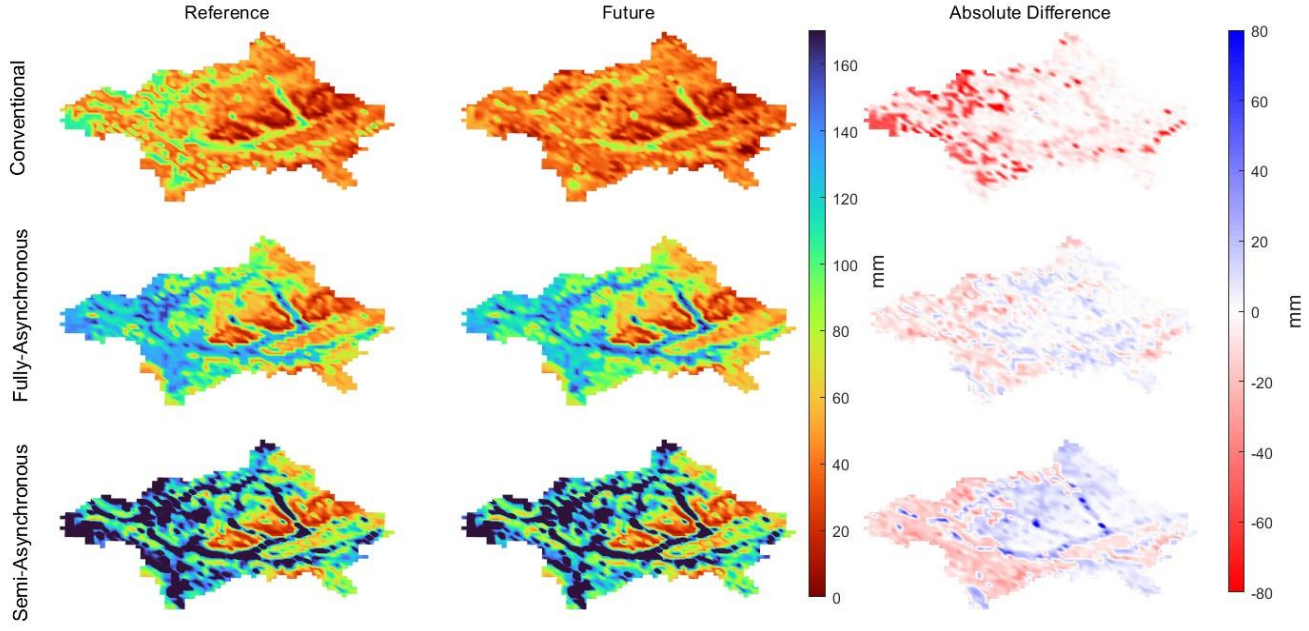

Figure 8. Spatial distribution of annual groundwater recharge in the Matane catchment for the reference period (1981–2010) and future period (2070–2099).

Figure 9 illustrates the spatial distribution of soil moisture across the Matane catchment for both the reference period (1981–2010) and the future period (2070–2099), comparing results from the conventional, fully asynchronous and semi-asynchronous methods. All three methods demonstrate that soil moisture distribution is heavily influenced by soil type, as indicated by the consistent spatial patterns observed (detailed soil type information is provided in the Appendix E, Fig. E1). The soil moisture maps show that areas with finer soils, such as loam, tend to have higher moisture retention, while coarser soils, such as sandy loams, exhibit lower moisture levels.

The fully asynchronous method tends to generate slightly higher soil moisture values compared to the other two methods, particularly in areas with inherently higher moisture retention capacity. The fully asynchronous method also displays greater variability in soil moisture patterns.

In terms of absolute changes between the reference and future periods, the conventional and semi-asynchronous methods project a general decrease in soil moisture, predominantly in regions with initially higher moisture values. The fully asynchronous method, while also projecting a decrease in soil moisture around high moisture areas, shows a more complex pattern with small regions exhibiting increases in soil moisture. Finally, it is noteworthy that the patterns of groundwater and soil moisture during the reference and future periods are spatially consistent and exhibit similar trends.

https://doi.org/10.5194/egusphere-2025-4450
Preprint. Discussion started: 18 September 2025

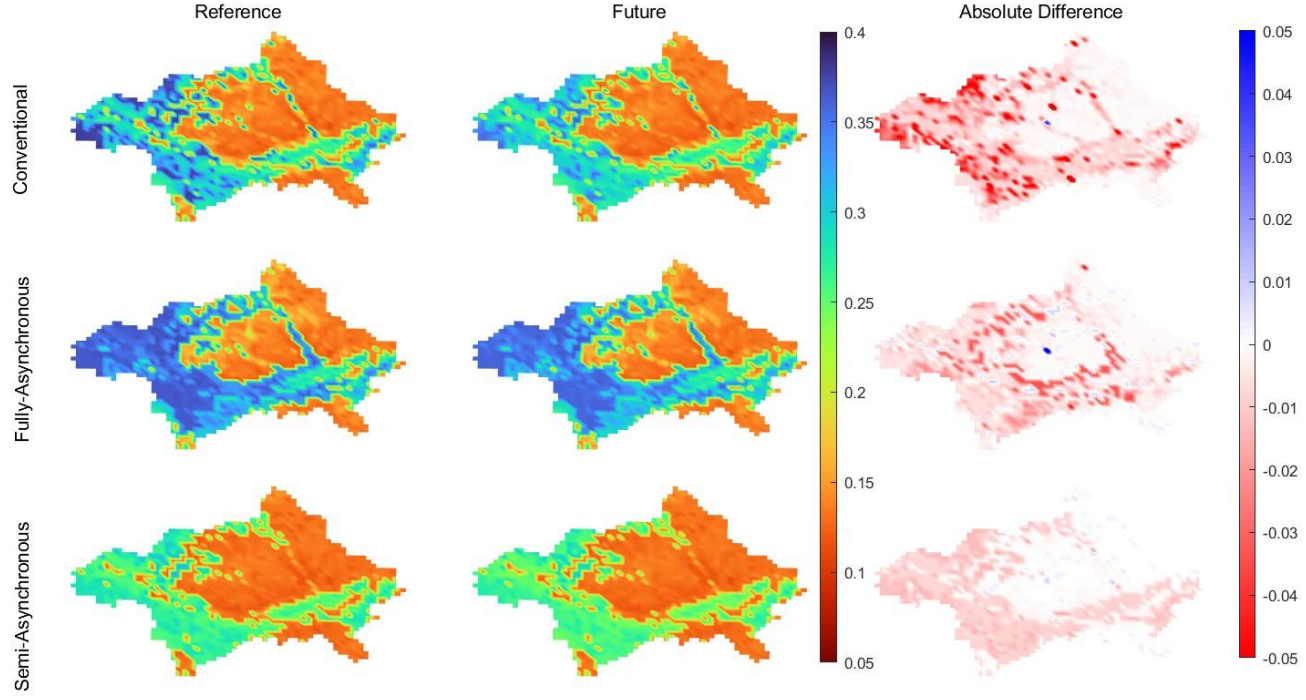

555 **Figure 9. Spatial distribution of soil moisture in the Matane catchment for the reference period (1981–2010) and future period (2070–2099).**

4 Discussion

The primary goal of this study was to evaluate the ability of the fully asynchronous and semi-asynchronous methods to reproduce key hydrological processes within catchments, in comparison to the conventional approach. By conducting detailed
560 analyses across ten catchments and focusing on a representative case study in the Matane catchment, the study assessed whether these alternative methods could serve as robust options for hydrological modeling in climate change impact studies. Particular attention was given to understanding how the introduction of a semi-asynchronous method, designed to improved seasonal timing, could address the limitations of the fully asynchronous method while maintaining its key advantages.

4.1 Hydroclimatic variable representation

565 One benefit of the fully asynchronous method is its ability to better represent extreme higher values (Q95) compared to conventional approach. By aligning the flow distribution with observed data, the fully asynchronous method effectively reproduces the magnitude of these high flow events, which is critical for managing flood risks under future climate conditions. However, despite its strengths in representing streamflow distributions, this study's findings align with other research indicating that the fully asynchronous method struggles to accurately capture the timing of observed streamflow, particularly
570 during spring high-flow events (Ricard et al., 2023). This issue contrasts with earlier findings by Ricard *et al.* (2020), who

https://doi.org/10.5194/egusphere-2025-4450
Preprint. Discussion started: 18 September 2025

reported that the fully asynchronous modeling approach provided a superior representation of the hydrologic regime compared to the conventional method. A key limitation of the current implementation of the fully asynchronous method arises from the use of RMSE as the objective function, which prioritizes matching the overall streamflow distribution rather than maintaining temporal coherence. While this approach successfully aligns streamflow percentiles with observed data, the lack of correlation between simulated and observed streamflow significantly affects the representation of key hydrological variables. Without proper synchronization, critical processes such as snowmelt timing and seasonal runoff contributions are misrepresented, leading to unrealistic hydrological dynamics. This discrepancy is particularly evident in snow-dominated catchments, where the fully asynchronous method tends to produce extended snowmelt periods and inconsistencies in peak flow timing.

The semi-asynchronous method helped mitigate this limitation by introducing a temporal structure during the calibration process, which improved the representation of seasonal dynamics and snowmelt timing, while still preserving much of the fully asynchronous method's strength in reproducing flow distributions.

The fully asynchronous and semi-asynchronous methods perform comparably to the conventional method when it comes to representing the spatial distribution of hydroclimatic variables such as soil moisture and groundwater recharge. This similarity is likely due to the strong correlation between these hydroclimatic variables and the physical properties of the catchment, such as elevation and soil type. The consistent representation of these variables across both methods suggests that the fundamental physical processes driving these patterns are well-captured, irrespective of the methodological differences in how streamflow is simulated. These conclusions are based on the spatial analysis of the Matane catchment. Future studies could extend this approach by analyzing multiple hydrological variables across multiple catchments to provide a broader understanding of spatial hydrological patterns.

The fully asynchronous and semi-asynchronous methods show consistency with the conventional method in predicting the long-term change for several variables, such as increases in precipitation and ETa, as well as decreases in SWE and snowfall. These findings align with broader climate change projections for the region, which anticipate warmer temperatures leading to reduced snow accumulation and altered precipitation patterns (Aygün *et al.*, 2022; Nolin *et al.*, 2023; Valencia Giraldo *et al.*, 2023). However, while the overall trends may appear consistent, the underlying processes and the accuracy of the projections differ significantly between the fully asynchronous and conventional methods.

Yet, a significant issue with the fully asynchronous method is its high sensitivity to variability in climate models. This problem comes from the biases inherent in climate models, which often lead to the simulation of hydrological processes occurring either too early or too late (Chen et al., 2021; Ricard et al., 2023). The fully asynchronous method, as currently implemented, adjust the calibration parameters to correct for biases, assuming that these biases remain constant over time. Consequently, if a climate model has significant or nonstationary biases, the fully asynchronous method will perpetuate these biases, leading to inaccuracies in the timing of peak flows and the representation of hydroclimatic variables. Ricard *et al.* (2023) also emphasize this vulnerability, noting that the fully asynchronous method is particularly prone to producing outlying projections due to the uncorrected biases in raw climate model outputs. They also suggest selecting climate models that exhibit the least hydrological bias to improve the reliability of fully asynchronous projections.

https://doi.org/10.5194/egusphere-2025-4450
Preprint. Discussion started: 18 September 2025

One of the most critical issues highlighted in this study is the concept of equifinality, where different models or methods achieve similar outcomes for different reasons (Mei et al., 2023; Yassin et al., 2017). In the case of the fully asynchronous method, it appears to replicate certain aspects of the conventional method's projections, but it does so through potentially flawed mechanisms.

By construction, the fully asynchronous method struggles to synchronize streamflow with the actual timing of hydrological events, particularly snowmelt. This lack of synchronization leads to a cascade of flawed mechanisms throughout the model. For instance, when snowmelt occurs too early or too late, the timing and magnitude of surface runoff are inaccurately represented, which can lead to unrealistic increases in surface runoff during inappropriate seasons. This misalignment also affects evapotranspiration and groundwater recharge, causing large, unrealistic variations, further skewing the model's output. Because the streamflow is not properly synchronized with the seasonal dynamics, the fully asynchronous method ultimately produces streamflow simulations that may match the overall distribution of the observations but do so for the wrong reasons. Equifinality becomes particularly problematic in this context because the fully asynchronous method may achieve similar projected changes in hydroclimatic variables as the conventional method, but for reasons that are not hydrologically sound. This brings into question the reliability of its projections, especially when the method demonstrates high variability among different climate models. Such variability, coupled with the method's inability to accurately replicate key hydrological processes, suggests that the fully asynchronous method, as implemented in this study, may not provide a robust framework for analyzing climate change impacts on hydroclimatic variables.

The semi-asynchronous method offers an innovative compromise that addresses key limitations of the fully asynchronous approach by integrating a monthly calibration strategy. This modification significantly improves the temporal alignment of key hydrological processes, particularly snowmelt timing, leading to a more coherent and physically realistic seasonal representation of streamflow and water balance components. Compared to the fully asynchronous method, the semi-asynchronous configuration exhibits reduced intermodel variability and avoids the pronounced misalignments seen in the representation of hydroclimatic variables.

Despite these improvements, the semi-asynchronous method remains sensitive to the biases inherent in raw climate model projections. Unlike the conventional method, which benefits from bias corrected climate model data, the semi asynchronous approach uses uncorrected data and must compensate internally for systemic errors. This contributes to a slightly higher variability in the reference period, although interestingly, the semi-asynchronous method maintains consistent variability between the reference and future periods. In contrast, the conventional method, while more stable in the reference period, shows an increase in intermodel variability in the future, likely due to differences between climate models in the magnitude of projected changes. This result suggests that preserving the original climate signal, as done in the semi-asynchronous method, may help maintain the ensemble's diversity, which can be advantageous for representing a broader range of possible futures, especially in the context of extremes.

Our findings show that introducing a mechanism to enforce temporal coherence between simulated and observed hydrological events, such as monthly calibration in the semi-asynchronous method, can lead to significant improvements in the simulation

https://doi.org/10.5194/egusphere-2025-4450
Preprint. Discussion started: 18 September 2025

of key hydrological processes. Without such a constraint, as in the fully asynchronous method, calibration retains excessive flexibility, often leading to physically implausible representations of hydrological processes and inconsistent seasonal behaviors. The semi-asynchronous method therefore represents a clear advancement over the fully asynchronous approach. It combines the benefit of preserving the raw climate model signal with improved process realism, making it a promising and innovative tool for climate change impact assessments. Furthermore, it stands as a legitimate alternative to the conventional method, offering a different trade-off between realism, variability, and the ability to capture extremes. By retaining the full spread of climate projections, unlike bias correction techniques that tend to smooth out extremes, it may provide a robust framework for evaluating the hydrological impacts of future extreme events.

4.2 Limitations and future directions

All three methods present distinct advantages and limitations. One of the most notable distinctions between the methods lies in how they handle extremes. The Multivariate Bias Correction (MBCn) approach, typically used in the conventional method, tends to dampen the extremes, smoothing out the peaks. In contrast, the fully asynchronous and semi-asynchronous methods, which calibrate directly on the distribution of streamflow without bias correction, preserve (or attempt to preserve) these extremes (Ricard et al., 2023). Maintaining extreme values may provide a more realistic representation of potential high-impact events.

Additionally, the selection of a bias correction method introduces another layer of uncertainty in hydrological projections. Studies have demonstrated that different correction techniques can significantly influence streamflow estimates, leading to variations in the magnitude and direction of projected hydrological impacts (Senatore et al., 2022; Chae and Chung, 2024). This added uncertainty highlights the challenge of determining the most appropriate correction approach, further emphasizing the importance of exploring alternative methods, such as asynchronous approaches, which eliminates the need for explicit bias correction.

One technical limitation of both the fully asynchronous and semi-asynchronous methods is the use of a scaling parameter during calibration, which adjusts the simulated streamflow by applying a constant ratio to match the observed mean. While these methods preserve the streamflow distribution and focus on relative changes, the use of a scaling adjustment prevents direct interpretation of absolute values of hydrological variables. As a result, these methods are primarily suited for evaluating relative changes over time rather than assessing the magnitude of future flows, which can be limiting for impact-based decision-making.

Another limitation of this study is the choice of meteorological data used to drive the hydrological simulations. While ERA5 was selected for its consistency and demonstrated reliability in previous studies, alternative datasets such as ERA5-Land or direct observations from weather stations could have influenced the results in terms of absolute values of change.

Another critical consideration is the computational demand of the fully asynchronous and semi-asynchronous methods. Due to their reliance calibration on every climate model, these methods require significantly more computational time in the calibration process. This increased computational cost must be weighed against the benefits of using the fully asynchronous

https://doi.org/10.5194/egusphere-2025-4450
Preprint. Discussion started: 18 September 2025

and semi-asynchronous methods, particularly when the conventional method might achieve similar results with less computational effort and more established reliability. Future work could explore strategies to reduce this computational burden, such as developing approaches specifically designed to optimize calibration time for the asynchronous framework.

The performance of the fully asynchronous method in snow-dominated catchments has proven to be problematic in this study. The method's inability to accurately capture snowmelt processes, as evidenced by the unrealistic snow retention and melt timing, casts doubt on its utility in regions where snow dynamics play a critical role in the hydrological cycle. Additionally, the high variability observed between climate models when using the fully asynchronous method suggests that the approach may be overly sensitive to the inherent uncertainties present in raw climate data. This variability complicates the interpretation of results and diminishes confidence in the method's projections, particularly in scenarios where precise predictions are required for decision-making.

The key takeaway from this study is that while the fully asynchronous method successfully preserves the distribution of streamflow and captures extreme events, it does so at the cost of increased intermodel variability and reduced accuracy in simulating critical hydrological processes, particularly those related to snow dynamics. These limitations make the fully asynchronous method less suitable for snow-dominated catchments, where precise representation of snowmelt timing and seasonal runoff is essential. In contrast, the semi-asynchronous method presents a clear improvement over the fully asynchronous approach by restoring temporal coherence and reducing inconsistencies in process representation. It also offers a legitimate alternative to the conventional method, preserving the raw climate model signal while delivering physically realistic hydrological simulations, which is particularly valuable for assessing the impacts of climate change on water resources.

Ultimately, these findings aim to inform decision-making in critical sectors such as agriculture, water resource management, urban planning, and environmental conservation. For example, soil moisture data is essential in agriculture for optimizing irrigation and improving crop yields, as well as in environmental management for maintaining wetlands and forest ecosystems. Groundwater recharge data supports sustainable management of aquifers, which is crucial for drinking water supplies, agriculture, and industrial use, while also guiding urban planning to avoid flooding or subsidence. Surface runoff modeling is vital for flood prevention and urban infrastructure design, ensuring stormwater systems can handle heavy rainfall. Lastly, streamflow data is key to water resource management, enabling efficient allocation for agriculture and industry, flood forecasting, and optimizing hydroelectric power generation. By providing detailed projections of these key hydroclimatic variables, this study supports adaptive management strategies across a wide range of sectors impacted by climate change.

Looking forward, further improvements could be made to the semi-asynchronous method by refining its monthly weighting strategy. Specifically, the α_m parameter, which controls the contribution of each month to the objective function, could be adjusted to assign different weights to different months. This would allow greater emphasis on critical periods, such as spring snowmelt or low-flow seasons, thereby improving the calibration's sensitivity to seasonal dynamics.

Future studies could also explore alternative calibration techniques, such as the Multiscale Parameter Regionalization (MPR) approach (Samaniego et al., 2010), which focuses on seamless parameter estimation across different spatial scales. Applying

https://doi.org/10.5194/egusphere-2025-4450
Preprint. Discussion started: 18 September 2025

MPR to WaSiM could improve parameter transferability and reduce the need for extensive calibration, potentially enhancing model robustness.

In parallel, ongoing advancements in climate modeling provide an opportunity to further refine the semi-asynchronous approach. As climate models become more accurate, with fewer biases and enhanced temporal precision, it would enable the semi-asynchronous method to offer more robust and reliable simulations of hydrological processes under future climate scenarios, positioning it as a more versatile tool for climate impact assessments.

5 Conclusion

This study evaluated the fully asynchronous and semi-asynchronous methods against the conventional method for assessing the impacts of climate change on hydrology, in order to simulate key hydrological variables under future climate scenarios. While the fully asynchronous method proved effective in preserving extreme streamflow values, it consistently struggled to capture the timing of hydrological events, particularly snowmelt. These timing mismatches led to unrealistic seasonal dynamics and introduced considerable variability across climate model outputs, limiting the method's reliability in regions where seasonal processes are critical.

The semi-asynchronous method proposed in this study was designed to address these shortcomings by introducing a monthly structure into the calibration process, aiming to balance the distributional strengths of the fully asynchronous approach with improved temporal coherence. As a result, it offers a more physically realistic representation of seasonal dynamics and reduces some of the inconsistencies observed in the fully asynchronous framework. While it still shows sensitivity to biases in uncorrected climate inputs and exhibits notable intermodel variability, the semi-asynchronous method stands as a promising and novel alternative to the conventional approach. It provides a different yet valuable trade-off between realism, ensemble diversity, and the ability to represent extreme events, making it a legitimate option for climate change impact assessments.

The conventional method delivered stable and hydrologically consistent simulations across catchments. Its reliance on bias-corrected climate data helps ensure a better alignment with observed seasonal dynamics. However, this robustness comes with certain limitations. By smoothing out variability and extremes through bias correction, the conventional method may limit the exploration of a wider range of plausible future scenarios. As a result, it offers less flexibility in representing the full diversity of climate model projections, which can be particularly important for assessing the risks associated with extreme events under climate change.

Future work should continue refining the semi-asynchronous method to improve its stability and applicability. In particular, adjusting the monthly weighting parameter (α_m) could allow the calibration process to focus more effectively on key periods such as snowmelt or low-flow seasons. Another important avenue for improvement lies in addressing the limitations introduced by the use of a scaling parameter, which constrains the interpretation of absolute values and restricts the method to relative change analysis. Exploring calibration strategies that remove the need for this scaling adjustment could enhance the semi-asynchronous method's utility for impact-based decision-making.

https://doi.org/10.5194/egusphere-2025-4450
Preprint. Discussion started: 18 September 2025

Appendix A

Table A1. List of GCMs along with their respective institutions and horizontal resolutions.

GCM Name	Institution	Resolution (lat. x lon.)
ACCESS-ESM1-5	Australian Community Climate and Earth System Simulator, Australia	1.25° x 1.875°
CMCC-ESM2	Centro Euro-Mediterraneo sui Cambiamenti Climatici, Italy	0.9° x 1.23°
CanESM5	Canadian Centre for Climate Modelling and Analysis, Canada	2.8° x 2.8°
EC-Earth3	European consortium of national meteorological services and research institutes; Spain, Denmark, Italy, Finland, Germany, Ireland, Portugal, Netherlands, Sweden, Norway, and Belgium.	~ 80 km
EC-Earth3-CC		~ 80 km
EC-Earth3-Veg-LR		~ 125 km
FGOALS-g3	Chinese Academy of Sciences, China	2.25° x 1.875°
GFDL-ESM4	Geophysical Fluid Dynamics Laboratory, USA	1° x 1.25°
INM-CM4-8	Institute for Numerical Mathematics, Russia	1.5° x 2°
INM-CM5-0		1.5° x 2°
IPSL-CM6A-LR	Institut Pierre Simon Laplace, France	1.26° x 2.5°
MIROC6	Japan Agency for Marine-Earth Science and Technology, Japan	1.4° x 1.4°
MPI-ESM1-2-HR	Max Planck Institute for Meteorology, Germany	0.9375° x 0.9375°
MPI-ESM1-2-LR		1.875° x 1.875°
MRI-ESM2-0	Meteorological Research Institute, Japan	1.125° x 1.125°
NESM3	Nanjing University of Information Science and Technology, China	1.875° x 1.875°
NorESM2-LM	Norwegian Climate Centre, Norway	1.875° x 2.5°
NorESM2-MM		0.9375° x 1.25°

https://doi.org/10.5194/egusphere-2025-4450
Preprint. Discussion started: 18 September 2025

Table A2. Monthly precipitation bias (%) between 18 global climate models (GCMs) and ERA5 reanalysis data for the reference period (1981-2010). Values represent the average bias across the 10 catchments included in the study. Monthly biases are shown for January (J) through December (D), with the final column indicating the annual mean bias for each model.

	Monthly precipitation bias (%)												
GCM	**J**	**F**	**M**	**A**	**M**	**J**	**J**	**A**	**S**	**O**	**N**	**D**	**Mean**
ACCESS-ESM1-5	14.1	22.1	29.6	2.5	13.7	12.6	23.4	11.2	-16.2	-16.3	-1.8	8.2	**8.6**
CMCC-ESM2	-12.1	7.3	-6.8	-14.7	-12.8	-11.1	-0.9	-14.9	-16.4	-11.0	-2.1	-9.2	**-8.7**
CanESM5	-10.3	0.6	-2.0	-6.6	16.5	23.9	36.2	26.6	22.0	5.4	-4.8	-23.4	**7.0**
EC-Earth3	-1.3	26.1	26.7	-2.6	1.6	8.3	0.7	-6.9	-7.5	3.6	3.0	-2.4	**4.1**
EC-Earth3-CC	-0.5	37.2	18.3	5.0	11.3	8.5	0.4	-9.5	13.8	11.7	7.4	-0.5	**8.6**
EC-Earth3-Veg-LR	-2.0	10.6	11.1	-11.3	4.6	-0.4	-3.6	-12.4	1.1	6.0	-2.1	-4.3	**-0.2**
FGOALS-g3	-3.8	-11.8	-7.3	-29.0	-38.9	-32.5	-22.1	-17.1	-23.0	-13.9	-1.5	3.7	**-16.4**
GFDL-ESM4	-5.9	12.2	3.2	-0.7	1.5	18.5	11.1	0.7	7.3	7.8	-1.0	-16.4	**3.2**
INM-CM4-8	20.5	22.6	26.0	-5.6	11.0	9.0	13.6	9.3	-18.3	-0.6	11.2	20.1	**9.9**
INM-CM5-0	18.1	18.7	16.0	-0.8	9.7	12.5	23.5	11.2	-8.2	-16.1	15.2	6.6	**8.9**
IPSL-CM6A-LR	27.2	39.6	31.4	0.3	8.4	16.2	34.5	28.4	10.7	-1.7	3.1	12.1	**17.5**
MIROC6	17.2	17.2	3.9	-13.5	16.9	27.8	22.1	10.1	-4.7	9.2	3.3	-4.6	**8.7**
MPI-ESM1-2-HR	-4.3	14.4	24.9	22.9	20.2	13.3	12.9	1.2	1.4	9.8	4.6	-18.7	**8.5**
MPI-ESM1-2-LR	-4.0	11.9	15.5	-0.8	6.9	10.5	22.0	-12.0	8.0	-10.1	-6.4	-17.9	**2.0**
MRI-ESM2-0	-8.7	2.6	-3.0	-10.0	-0.1	8.3	10.3	-6.5	0.3	0.6	-4.6	5.8	**-0.4**
NESM3	0.7	38.6	36.1	10.1	8.0	7.9	17.9	5.5	-9.5	-8.9	1.2	-13.4	**7.8**
NorESM2-LM	-16.5	1.7	-9.3	-25.1	-22.8	-10.9	-23.9	-23.2	-12.2	-15.9	-18.5	-20.1	**-16.4**
NorESM2-MM	-10.9	-6.5	-3.3	-23.7	-20.2	-7.4	-15.4	-26.1	-20.0	-18.4	-5.0	-5.8	**-13.5**

https://doi.org/10.5194/egusphere-2025-4450
Preprint. Discussion started: 18 September 2025

Table A3. Monthly temperature bias (°C) between 18 global climate models (GCMs) and ERA5 reanalysis data for the reference period (1981-2010). Values represent the average bias across the 10 catchments included in the study. Monthly biases are shown for January (J) through December (D), with the final column indicating the annual mean bias for each model.

	Monthly temperature bias (°C)												
GCM	**J**	**F**	**M**	**A**	**M**	**J**	**J**	**A**	**S**	**O**	**N**	**D**	**Mean**
ACCESS-ESM1-5	4.4	2.3	2.6	1.3	-0.3	0.1	0.6	0.4	0.9	1.5	1.4	4.1	**1.6**
CMCC-ESM2	0.0	-0.2	0.6	0.5	0.0	-0.3	0.3	0.2	0.7	1.2	0.7	0.3	**0.3**
CanESM5	0.1	-0.3	0.9	1.6	2.6	2.0	1.4	1.9	1.4	0.8	-0.2	-0.4	**1.0**
EC-Earth3	-2.2	-1.7	-2.2	-3.5	-4.6	-3.0	-2.2	-1.0	-0.2	-0.7	-0.9	-1.5	**-2.0**
EC-Earth3-CC	-1.3	0.2	-1.5	-2.3	-3.1	-2.1	-1.2	-0.4	0.4	0.6	-1.0	-1.2	**-1.1**
EC-Earth3-Veg-LR	-3.2	-4.1	-2.7	-3.5	-4.3	-3.4	-1.4	-0.6	0.5	0.0	-1.6	-2.6	**-2.2**
FGOALS-g3	-1.2	-2.0	-0.7	0.0	-1.1	-0.6	0.2	0.1	-0.9	-0.3	-0.2	-0.4	**-0.6**
GFDL-ESM4	-0.6	0.1	-1.3	-2.0	-2.6	-1.9	-1.9	-1.9	-1.5	-1.0	-1.8	-0.6	**-1.4**
INM-CM4-8	-1.2	-0.7	-1.2	-0.3	1.5	0.8	0.7	0.6	0.7	1.8	1.8	0.5	**0.4**
INM-CM5-0	-2.4	-3.1	-3.6	-2.9	0.3	0.5	0.5	0.1	0.1	1.8	1.4	-0.8	**-0.7**
IPSL-CM6A-LR	-2.0	-1.5	-1.7	-1.9	-0.4	1.0	2.0	2.7	1.4	0.2	-1.2	-1.8	**-0.3**
MIROC6	2.5	1.1	0.0	0.1	1.9	2.5	2.7	2.3	2.4	2.3	1.7	1.7	**1.8**
MPI-ESM1-2-HR	0.3	-1.1	-1.8	-1.0	-0.1	0.0	-0.4	-0.4	0.0	-0.2	-0.6	0.2	**-0.4**
MPI-ESM1-2-LR	-1.1	-2.1	-2.4	-1.3	0.0	-0.4	-0.5	-0.8	-0.3	-0.1	-1.5	-1.0	**-1.0**
MRI-ESM2-0	-0.5	-0.4	-0.2	-0.4	-0.8	-0.3	0.5	0.3	0.1	-0.6	-1.0	0.0	**-0.3**
NESM3	-1.1	-1.8	-2.0	-1.3	-0.2	0.4	1.4	1.5	1.9	0.5	-1.7	-1.5	**-0.3**
NorESM2-LM	1.3	-0.8	-1.0	-1.3	-2.7	-2.0	0.3	1.5	1.1	0.9	1.0	1.7	**0.0**
NorESM2-MM	-0.3	-1.0	-0.8	-1.8	-2.6	-1.3	0.6	0.4	0.6	0.7	0.5	0.4	**-0.4**

https://doi.org/10.5194/egusphere-2025-4450
Preprint. Discussion started: 18 September 2025

Appendix B

Table B1. Kling-Gupta Efficiency (KGE) values for the conventional method during the calibration and validation periods across ten catchments. The mean KGE values for calibration and validation are also provided.

Conventional Method		**KGE**	
Name	Area (km^2)	Calibration	Validation
Bonaventure	1910	0.847	0.889
Matane	1650	0.906	0.906
Ouelle	795	0.894	0.834
Bécancour	919	0.850	0.807
Nicolet Sud-Ouest	549	0.817	0.786
Au Saumon	738	0.831	0.778
Bras du Nord	642	0.873	0.872
Du Loup	774	0.838	0.804
Valin	746	0.902	0.885
Godbout	1570	0.869	0.863
	Mean	0.863	0.842

Table B2. Root Mean Square Error (RMSE) values calculated using sorted simulated and observed streamflow during the calibration and validation periods across ten catchments. The mean RMSE values for calibration and validation are also provided.

RMSE	**Asynchronous**				**Semi-Asynchronous**				**Conventional**	
Name	Calibration		Validation		Calibration		Validation		Calibration	Validation
	Mean	Std	Mean	Std	Mean	Std	Mean	Std		
Bonaventure	*0.108*	*0.030*	*0.151*	*0.045*	*0.276*	*0.070*	*0.256*	*0.062*	*0.465*	*0.296*
Matane	*0.124*	*0.021*	*0.180*	*0.034*	*0.319*	*0.089*	*0.334*	*0.130*	*0.439*	*0.279*
Ouelle	*0.125*	*0.027*	*0.167*	*0.043*	*0.315*	*0.085*	*0.308*	*0.092*	*0.180*	*1.362*
Bécancour	*0.095*	*0.019*	*0.158*	*0.048*	*0.252*	*0.055*	*0.255*	*0.072*	*0.976*	*0.295*
Nicolet Sud-Ouest	*0.125*	*0.034*	*0.200*	*0.097*	*0.297*	*0.048*	*0.263*	*0.073*	*0.320*	*0.925*
Au Saumon	*0.156*	*0.054*	*0.209*	*0.053*	*0.390*	*0.078*	*0.385*	*0.075*	*0.824*	*0.614*
Bras du Nord	*0.175*	*0.044*	*0.243*	*0.063*	*0.283*	*0.105*	*0.314*	*0.151*	*0.425*	*0.361*
Du Loup	*0.085*	*0.019*	*0.165*	*0.091*	*0.201*	*0.037*	*0.228*	*0.066*	*0.360*	*0.232*
Valin	*0.109*	*0.036*	*0.162*	*0.055*	*0.258*	*0.046*	*0.264*	*0.062*	*0.333*	*0.325*
Godbout	*0.110*	*0.032*	*0.157*	*0.037*	*0.231*	*0.042*	*0.239*	*0.036*	*0.645*	*0.493*
Mean	0.121	0.031	0.179	0.057	0.282	0.065	0.285	0.082	0.497	0.518

https://doi.org/10.5194/egusphere-2025-4450
Preprint. Discussion started: 18 September 2025

Appendix C

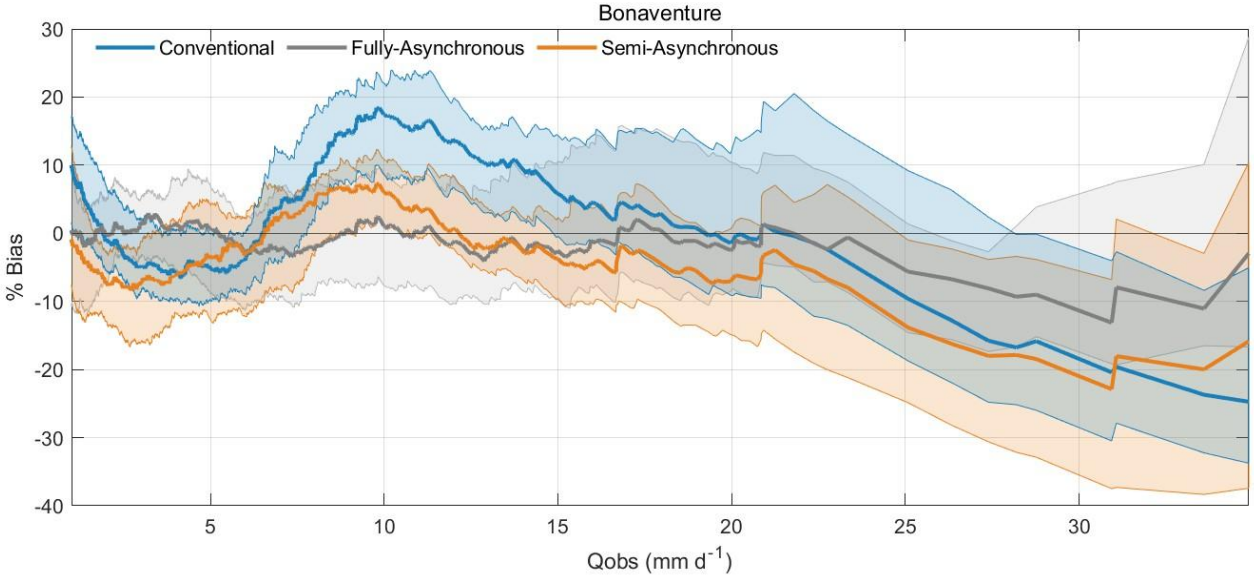

Figure C1. Performance comparison between the conventional, fully asynchronous and semi-asynchronous methods for the Bonaventure catchment during the reference period (1981–2010). The figure shows the percentage bias between observed and simulated streamflows, with the x-axis representing the observed daily streamflow and the y-axis displaying the percentage bias relative to the observed values. The shaded regions illustrate the variability among climate models around the mean bias for each method.

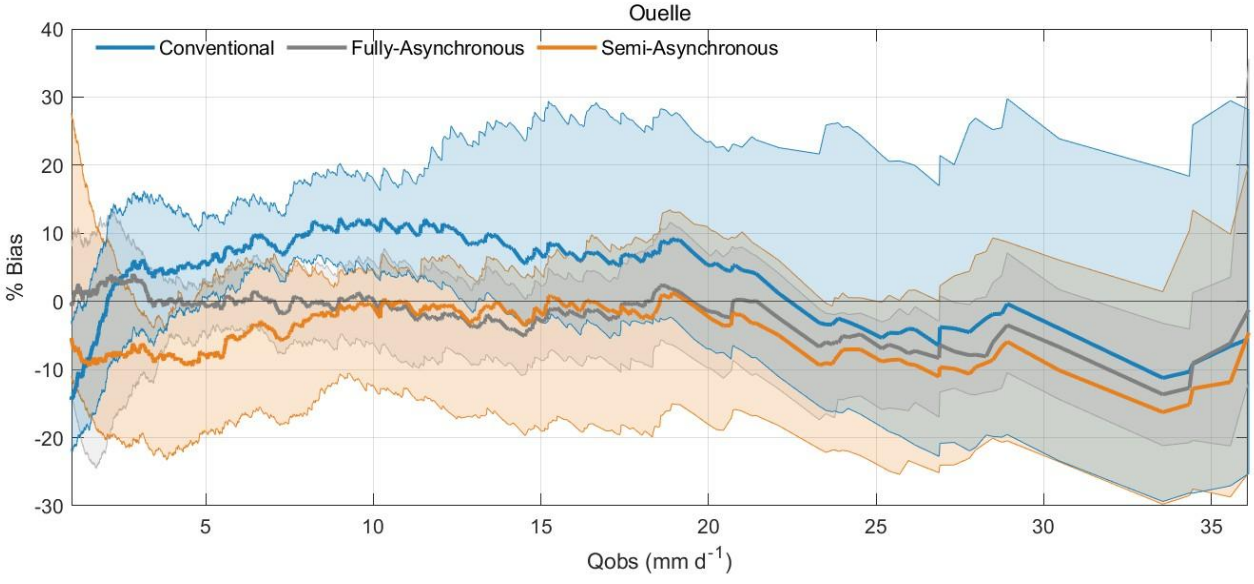

Figure C2. Same as Fig. C1, but for Ouelle catchment.

https://doi.org/10.5194/egusphere-2025-4450
Preprint. Discussion started: 18 September 2025

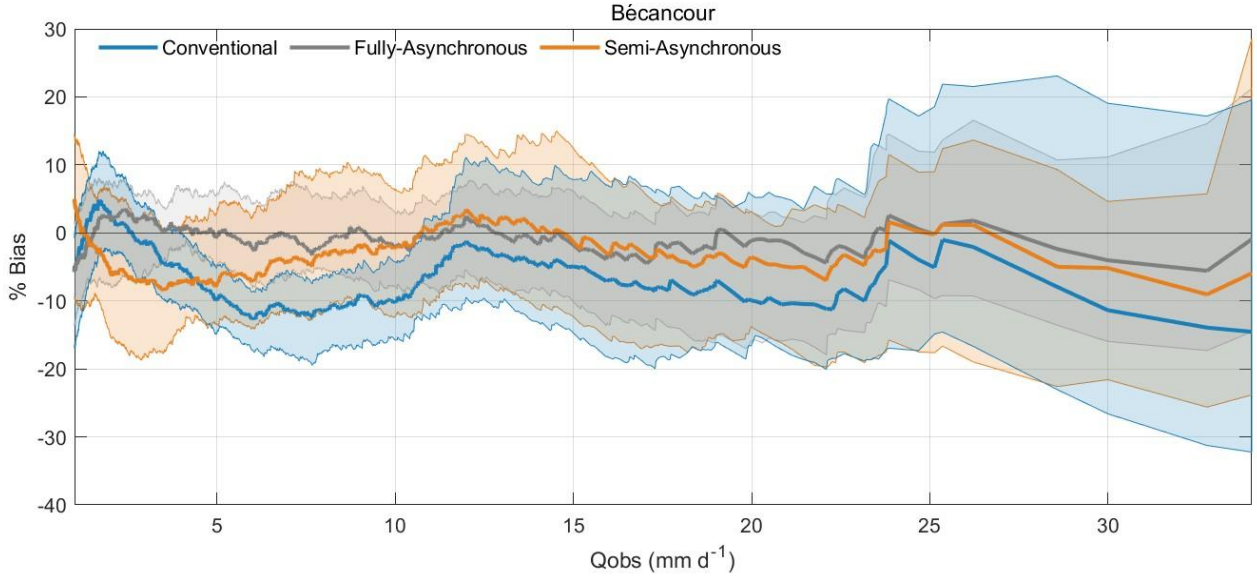

Figure C3. Same as Fig. C1, but for Bécancour catchment.

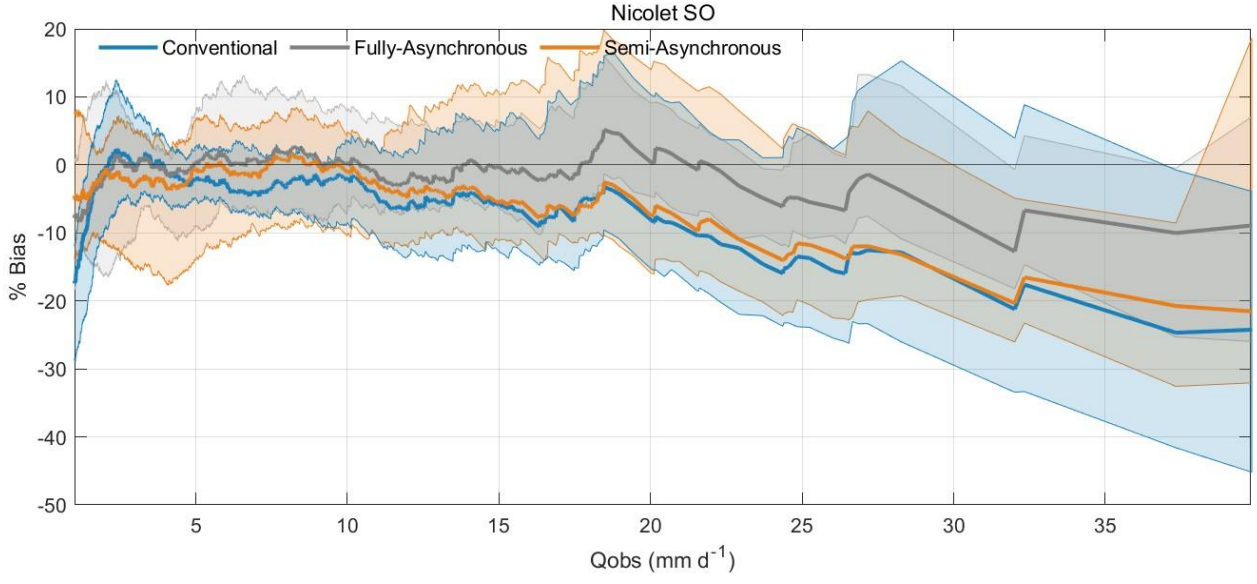

770 **Figure C4. Same as Fig. C1, but for Nicolet Sud-Ouest catchment.**

https://doi.org/10.5194/egusphere-2025-4450
Preprint. Discussion started: 18 September 2025

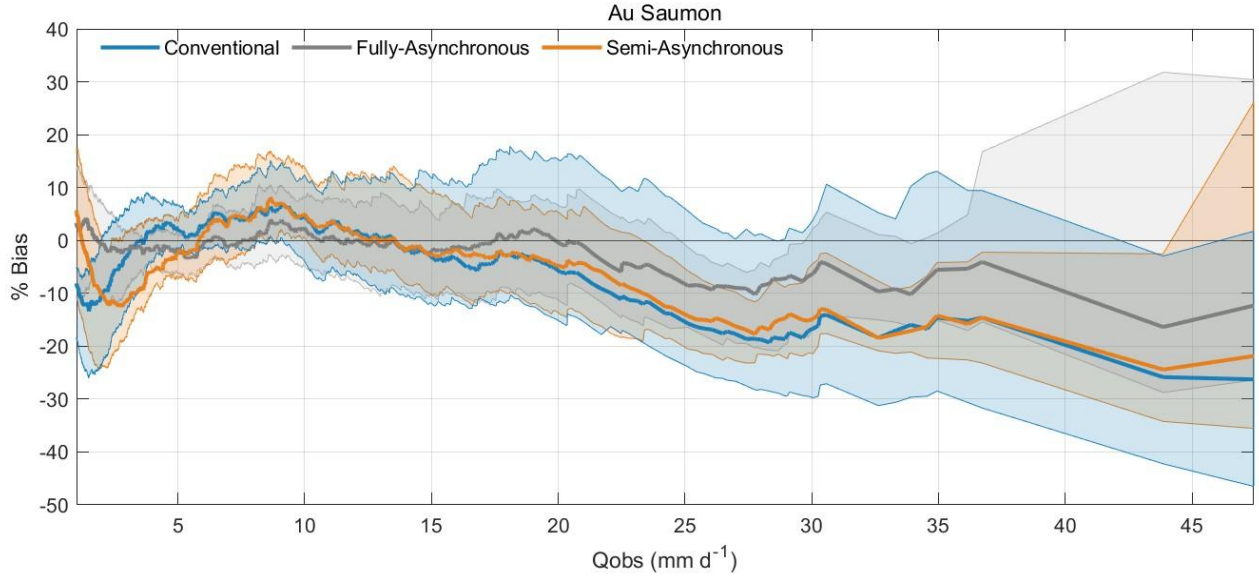

Figure C5. Same as Fig. C1, but for Au Saumon catchment.

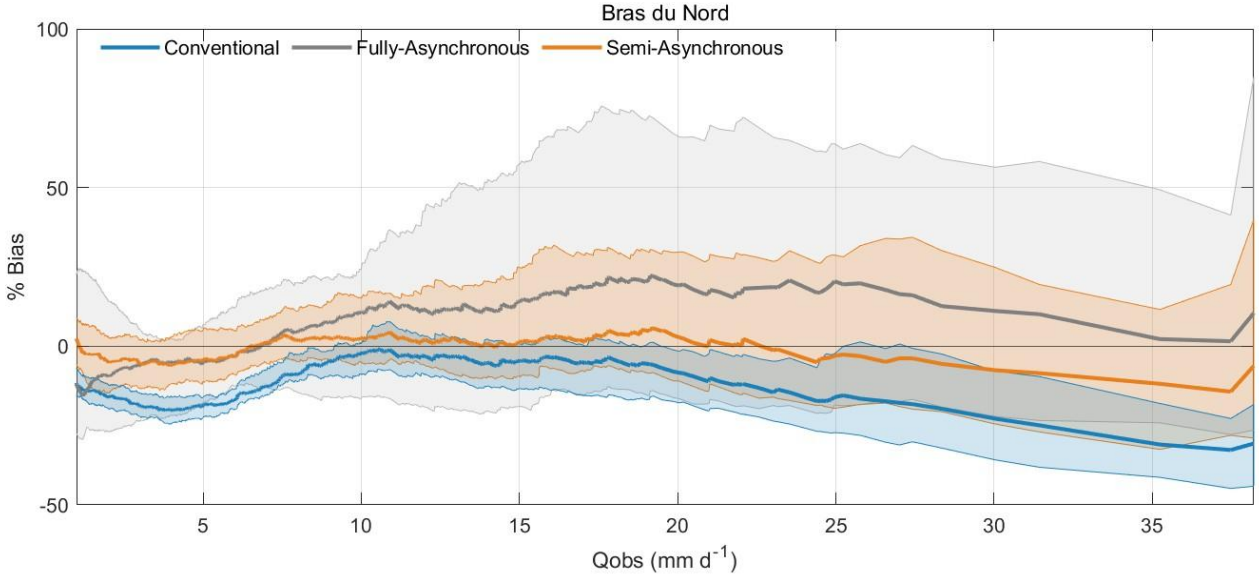

Figure C6. Same as Fig. C1, but for Bras du Nord catchment.

https://doi.org/10.5194/egusphere-2025-4450
Preprint. Discussion started: 18 September 2025

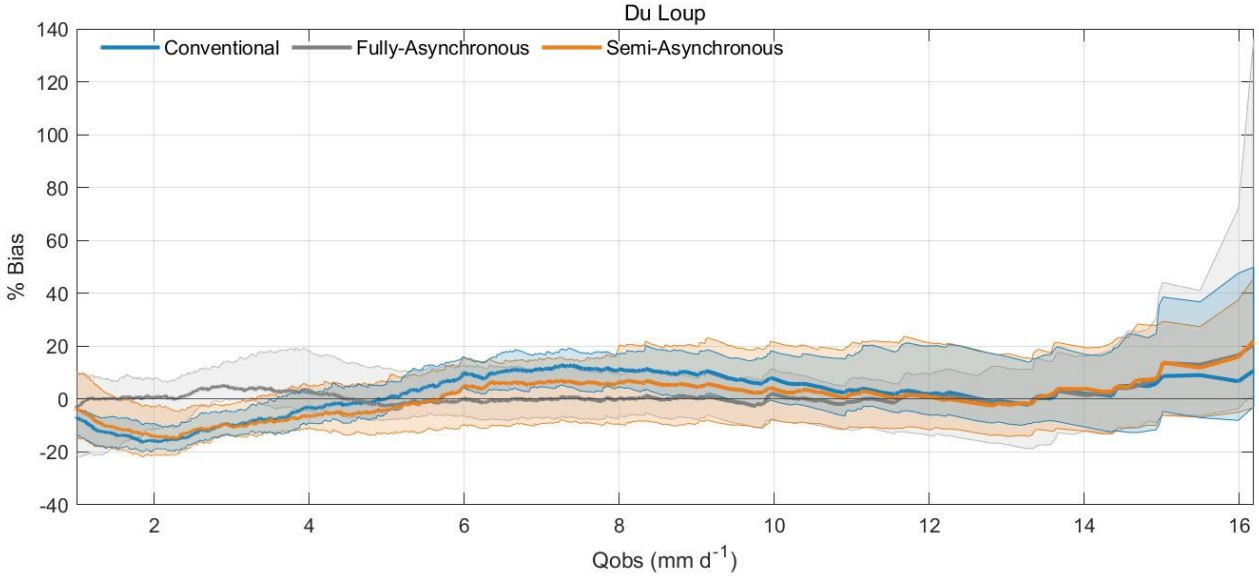

775

Figure C7. Same as Fig. C1, but for Du Loup catchment.

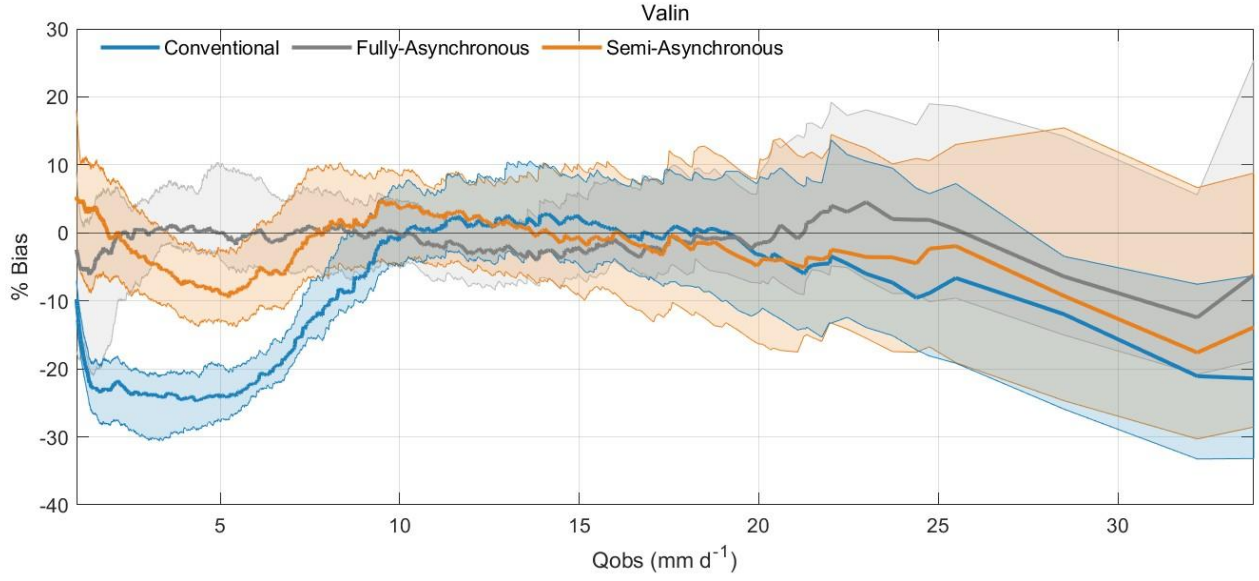

Figure C8. Same as Fig. C1, but for Valin catchment.

https://doi.org/10.5194/egusphere-2025-4450
Preprint. Discussion started: 18 September 2025

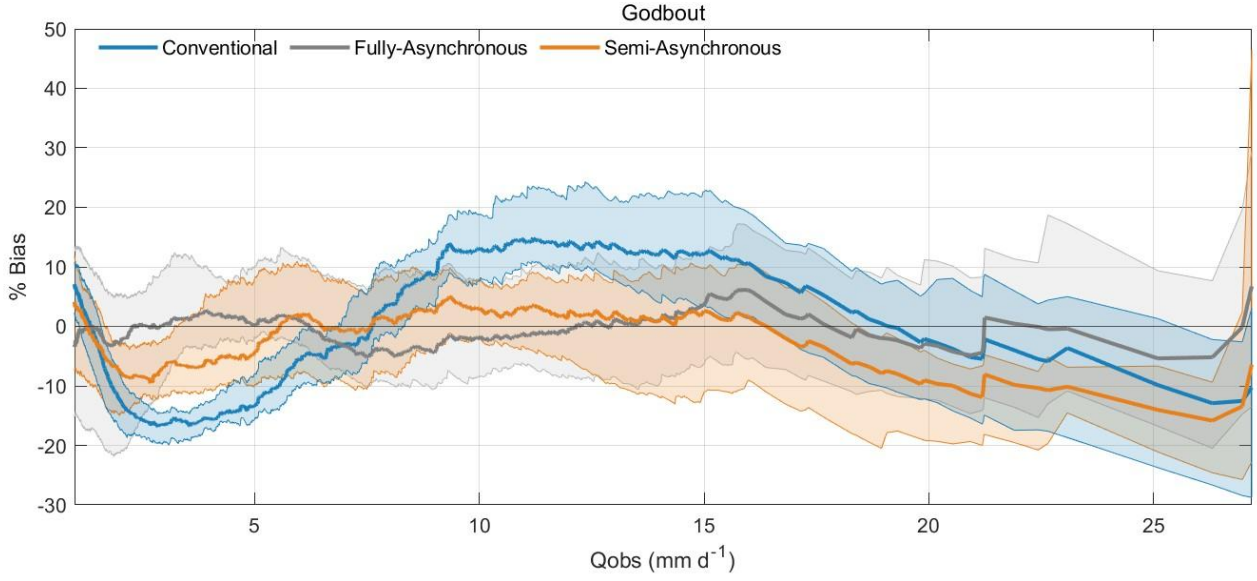

780 **Figure C9. Same as Fig. C1, but for Godbout catchment.**

785

790

795

https://doi.org/10.5194/egusphere-2025-4450
Preprint. Discussion started: 18 September 2025

Appendix D

Table D1. Analysis of Q95% streamflow distribution across 10 catchments for the reference and future periods. Metrics include the median (med) and standard deviation (std) of Q95% values (%).

Q95%

Catchment Name			Bonaventure	Matane	Ouelle	Bécancour	Nicolet SO	Au Saumon	Bras du Nord	Du Loup	Valin	Godbout	Absolute Mean
Reference Period	**Conv.**	**med (%)**	4.5	-4.2	6.8	-11.7	-3.4	4.8	-6.1	1.1	-6.7	2.5	**5.2**
		std (%)	4.1	3.2	3.3	3.1	2.7	4.5	2.3	3.1	3.4	3.9	**3.4**
	Fully-asyn.	**med (%)**	0.3	-0.3	1.6	-0.6	4.1	2.3	-12.8	-0.1	1.6	-3.0	**2.7**
		std (%)	4.1	4.1	3.0	3.4	7.2	4.0	25.4	3.2	3.4	3.9	**6.2**
	Semi-asyn.	**med (%)**	2.2	-5.1	-5.5	-3.7	0.2	4.6	2.4	-3.2	1.7	1.4	**3.0**
		std (%)	4.1	5.1	5.6	5.2	4.2	4.4	5.0	4.9	4.4	4.7	**4.8**
Projected Change	**Conv.**	**med (%)**	-15.8	-16.7	-20.0	-7.2	-17.6	-16.6	-12.4	-8.3	-9.8	-6.0	**13.0**
		std (%)	10.4	13.7	11.1	9.1	7.3	9.0	8.9	7.9	10.9	10.9	**9.9**
	Fully-asyn.	**med (%)**	-15.0	-11.0	-8.7	-6.2	-10.2	-14.1	-3.1	-6.7	-3.3	-5.0	**8.4**
		std (%)	8.0	7.9	12.7	7.3	11.2	10.9	9.3	11.6	10.0	11.1	**10.0**
	Semi-asyn.	**med (%)**	-9.6	-22.6	-1.7	-8.2	10.8	-1.3	-23.4	25.3	-13.4	-9.0	**12.5**
		std (%)	19.8	11.6	25.0	18.8	26.6	20.2	9.5	19.5	8.8	10.9	**17.1**

Table D2. Same as D1, but for Q50%.

Q50%

Catchment Name			Bonaventure	Matane	Ouelle	Bécancour	Nicolet SO	Au Saumon	Bras du Nord	Du Loup	Valin	Godbout	Absolute Mean
Reference Period	**Conv.**	**med (%)**	12.8	-11.3	-15.0	-3.3	-20.5	-9.0	-13.9	-1.5	-23.4	2.4	**11.3**
		std (%)	3.6	3.3	4.0	4.7	4.5	4.5	2.5	2.6	2.3	2.7	**3.5**
	Fully-asyn.	**med (%)**	2.2	-5.0	-5.3	-3.2	-7.1	6.1	-24.3	-2.1	-1.0	1.4	**5.8**
		std (%)	6.6	6.0	6.5	7.1	6.5	7.1	28.8	10.0	7.9	10.9	**9.7**
	Semi-asyn.	**med (%)**	2.2	2.4	6.5	1.8	-2.9	4.5	-2.5	0.7	2.1	1.2	**2.7**
		std (%)	6.1	4.8	10.6	5.3	6.6	7.7	5.5	5.6	5.3	5.0	**6.2**
Projected Change	**Conv.**	**med (%)**	15.8	18.7	25.2	18.4	18.2	13.0	17.8	14.9	23.5	14.6	**18.0**
		std (%)	16.6	25.3	24.1	16.7	20.2	15.7	15.1	15.8	18.5	16.0	**18.4**
	Fully-asyn.	**med (%)**	3.9	11.0	20.7	20.5	9.0	3.3	17.2	16.3	19.0	22.8	**14.4**
		std (%)	29.9	16.0	16.3	13.8	17.6	18.4	15.2	19.4	13.8	17.9	**17.8**
	Semi-asyn.	**med (%)**	53.9	17.4	30.9	15.3	40.6	8.0	-3.1	66.4	5.6	35.0	**27.6**
		std (%)	41.3	24.9	36.3	31.1	32.3	31.4	19.2	34.2	17.2	24.1	**29.2**

https://doi.org/10.5194/egusphere-2025-4450
Preprint. Discussion started: 18 September 2025

805

Table D3. Same as D1, but for Q5%.

Q5%

Catchment Name			Bonaventure	Matane	Ouelle	Bécancour	Nicolet SO	Au Saumon	Bras du Nord	Du Loup	Valin	Godbout	Absolute Mean
Reference Period	**Conv.**	**med (%)**	39.3	4.9	158.4	26.5	66.1	61.2	3.2	129.8	53.4	85.3	**62.8**
		std (%)	5.4	3.9	12.7	5.7	8.1	5.6	2.7	5.6	2.0	1.0	**5.3**
	Fully-asyn.	**med (%)**	12.0	34.2	137.6	42.5	109.9	31.7	-12.5	60.8	27.2	17.3	**48.6**
		std (%)	15.3	17.6	81.3	18.5	48.1	41.1	45.0	20.0	11.6	10.8	**30.9**
	Semi-asyn.	**med (%)**	42.4	45.6	275.4	103.8	160.7	93.6	24.4	117.1	49.5	41.5	**95.4**
		std (%)	14.9	18.1	72.8	25.8	36.6	46.0	10.2	15.1	14.9	8.4	**26.3**
Projected Change	**Conv.**	**med (%)**	-25.1	-32.5	-40.1	-25.2	-55.9	-26.3	3.7	-4.0	0.1	6.2	**21.9**
		std (%)	8.6	13.1	11.2	6.0	17.1	19.2	10.9	7.5	5.6	5.1	**10.4**
	Fully-asyn.	**med (%)**	-17.6	-8.4	1.3	14.4	-19.5	-24.1	-11.3	11.4	-12.2	17.2	**13.8**
		std (%)	30.5	20.9	21.5	19.1	27.4	28.8	19.1	22.6	27.7	37.8	**25.5**
	Semi-asyn.	**med (%)**	-0.4	-16.5	-17.9	-4.2	3.7	-34.3	-19.6	36.2	6.8	13.3	**15.3**
		std (%)	27.7	19.8	29.6	24.0	36.3	31.2	19.6	24.5	18.1	22.5	**25.3**

https://doi.org/10.5194/egusphere-2025-4450
Preprint. Discussion started: 18 September 2025

Appendix E

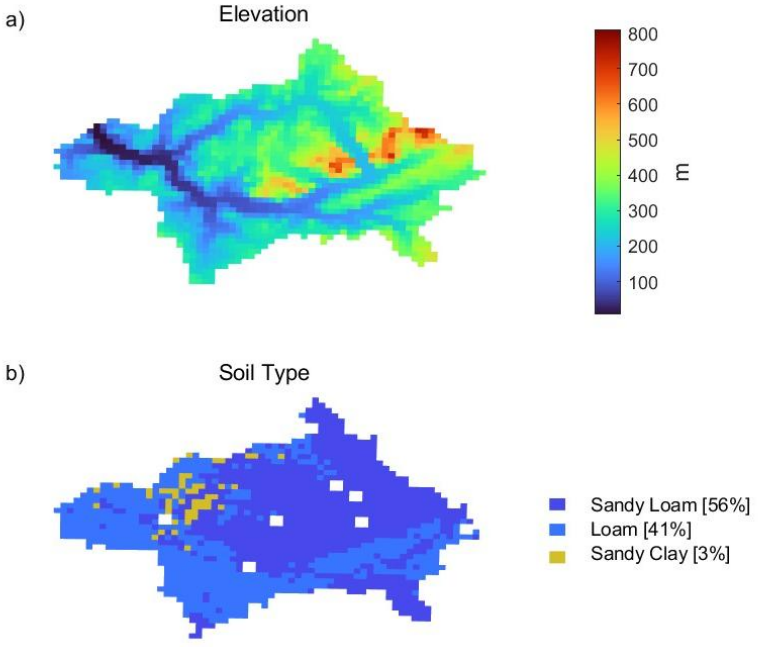

Figure E1. Topographic and soil type characteristics of the Matane catchment. Panel (a) shows the elevation map, with elevations ranging from 100 to 800 meters above sea level. Higher elevations are indicated in warmer colors (reds and oranges), while lower elevations are shown in cooler colors (blues and greens). Panel (b) displays the distribution of soil types within the catchment, with sandy loam covering 56% of the area (dark blue), loam covering 41% (light blue), and sandy clay occupying 3% (yellow).

https://doi.org/10.5194/egusphere-2025-4450
Preprint. Discussion started: 18 September 2025

Appendix F

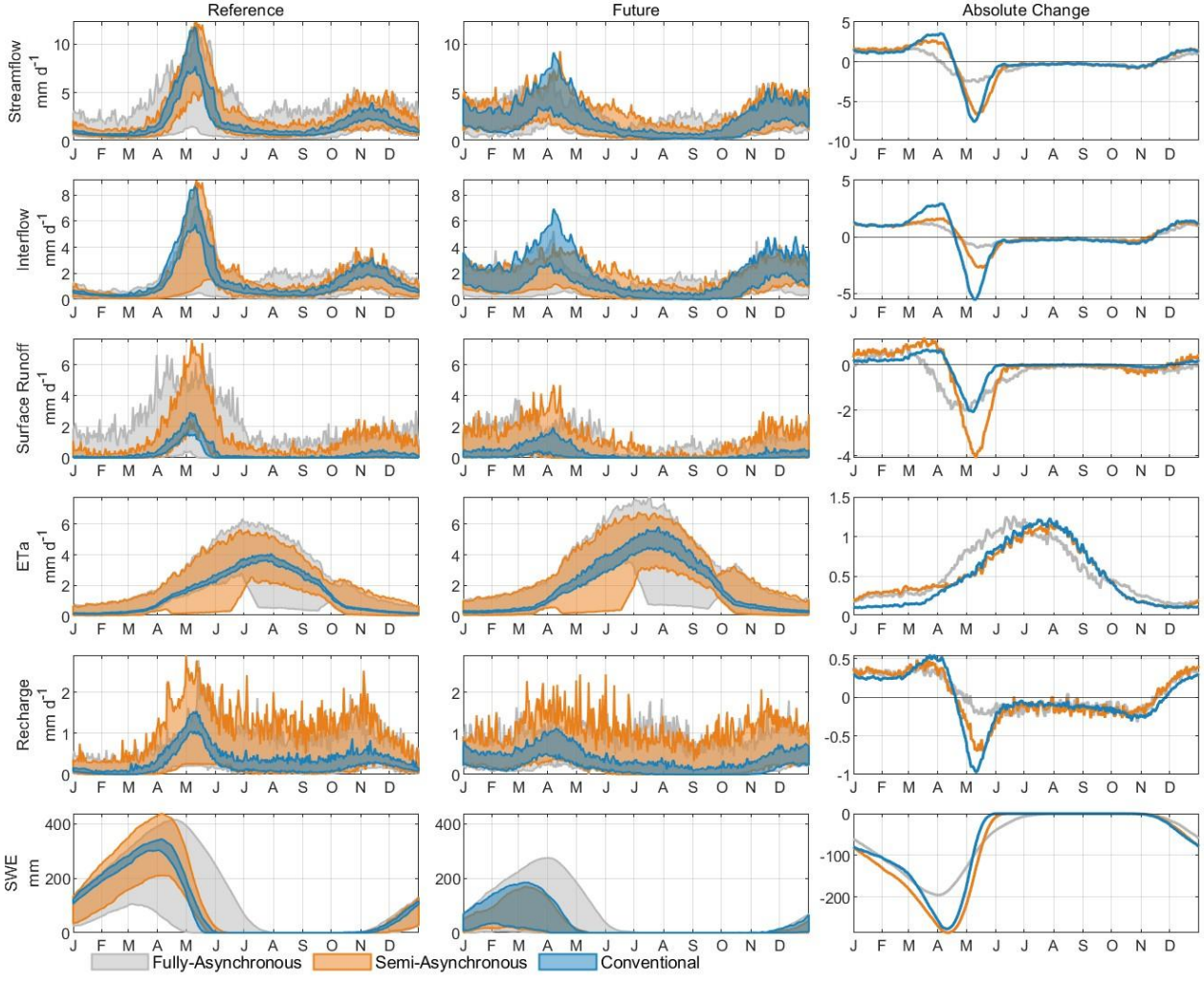

Figure F1. Seasonal distribution of key hydroclimatic variables for the reference period (1981–2010), future period (2070–2099), and their average absolute changes across the Bonaventure catchment.

https://doi.org/10.5194/egusphere-2025-4450
Preprint. Discussion started: 18 September 2025

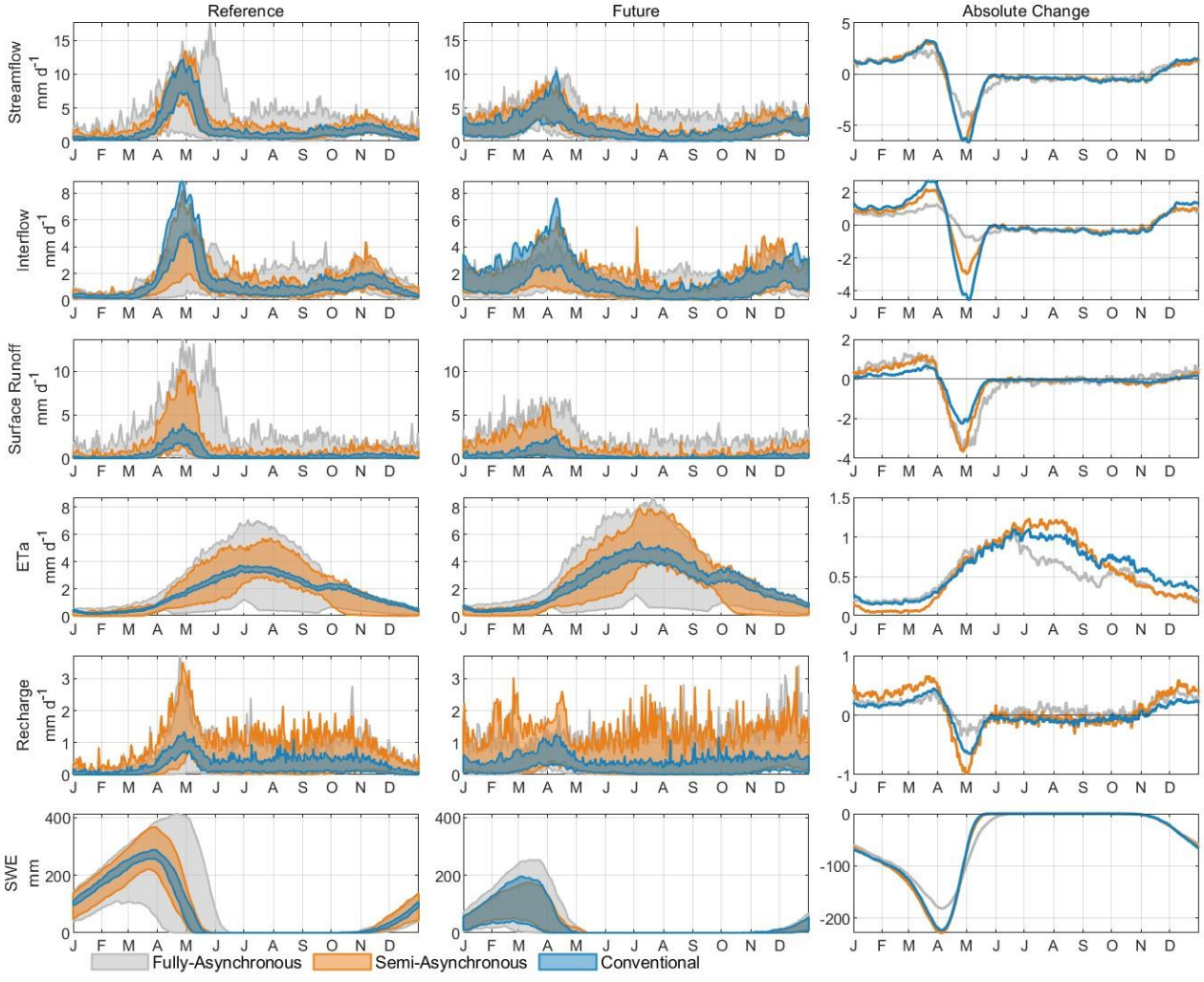

Figure F2. Same as F1, but for Ouelle catchment.

https://doi.org/10.5194/egusphere-2025-4450
Preprint. Discussion started: 18 September 2025

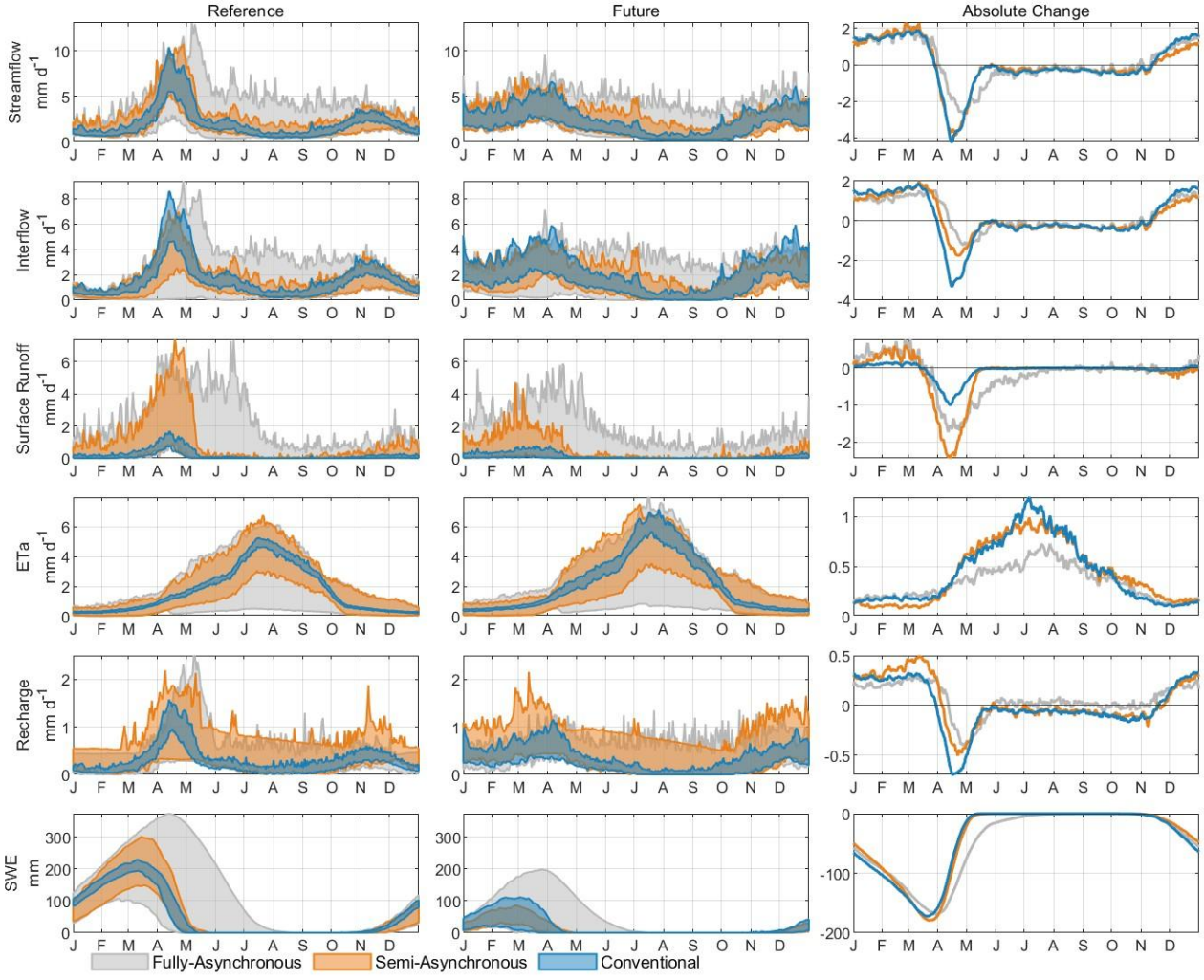

Figure F3. Same as F1, but for Bécancour catchment.

https://doi.org/10.5194/egusphere-2025-4450
Preprint. Discussion started: 18 September 2025

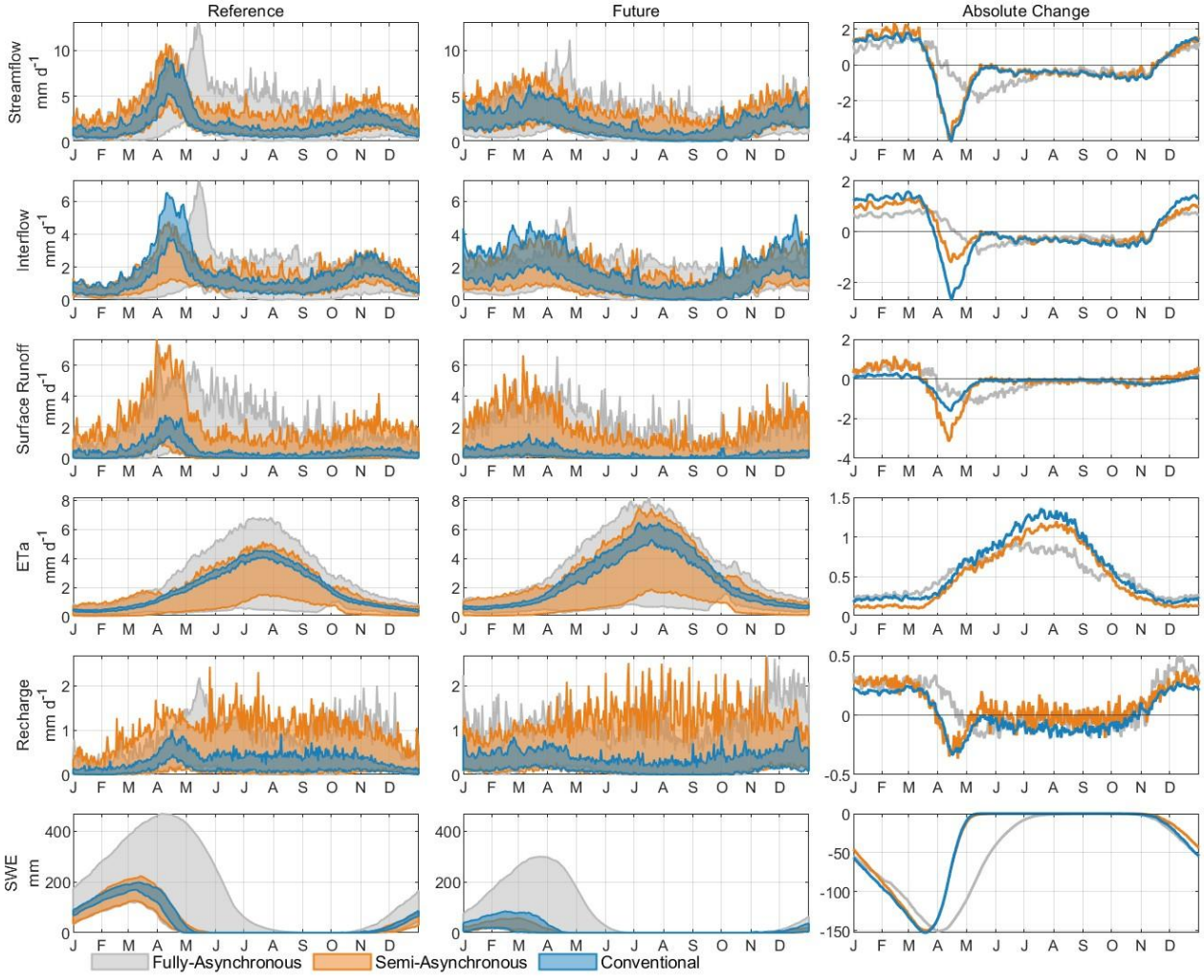

825 **Figure F4. Same as F1, but for Nicolet Sud-Ouest catchment.**

https://doi.org/10.5194/egusphere-2025-4450
Preprint. Discussion started: 18 September 2025

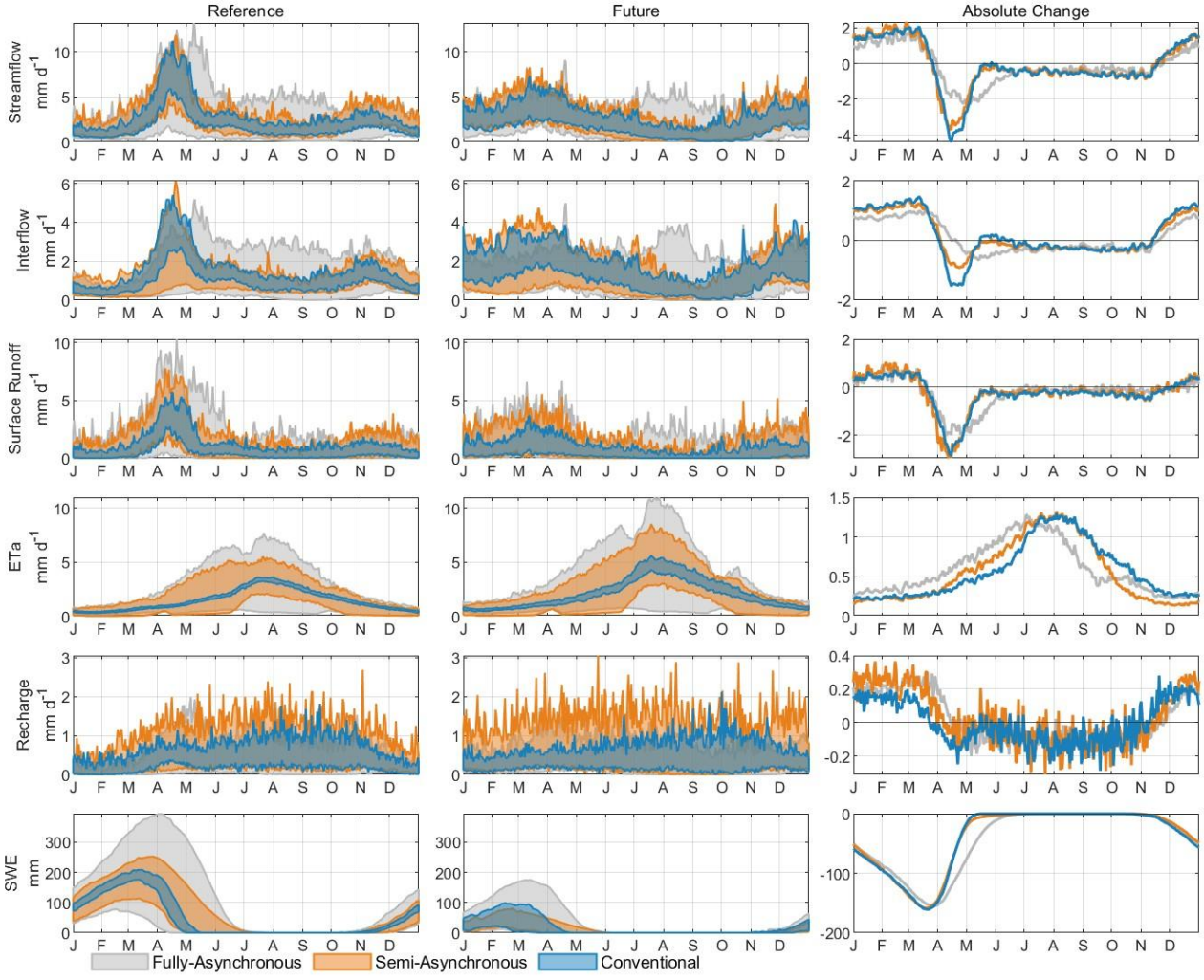

Figure F5. Same as F1, but for Au Saumon catchment.

https://doi.org/10.5194/egusphere-2025-4450
Preprint. Discussion started: 18 September 2025

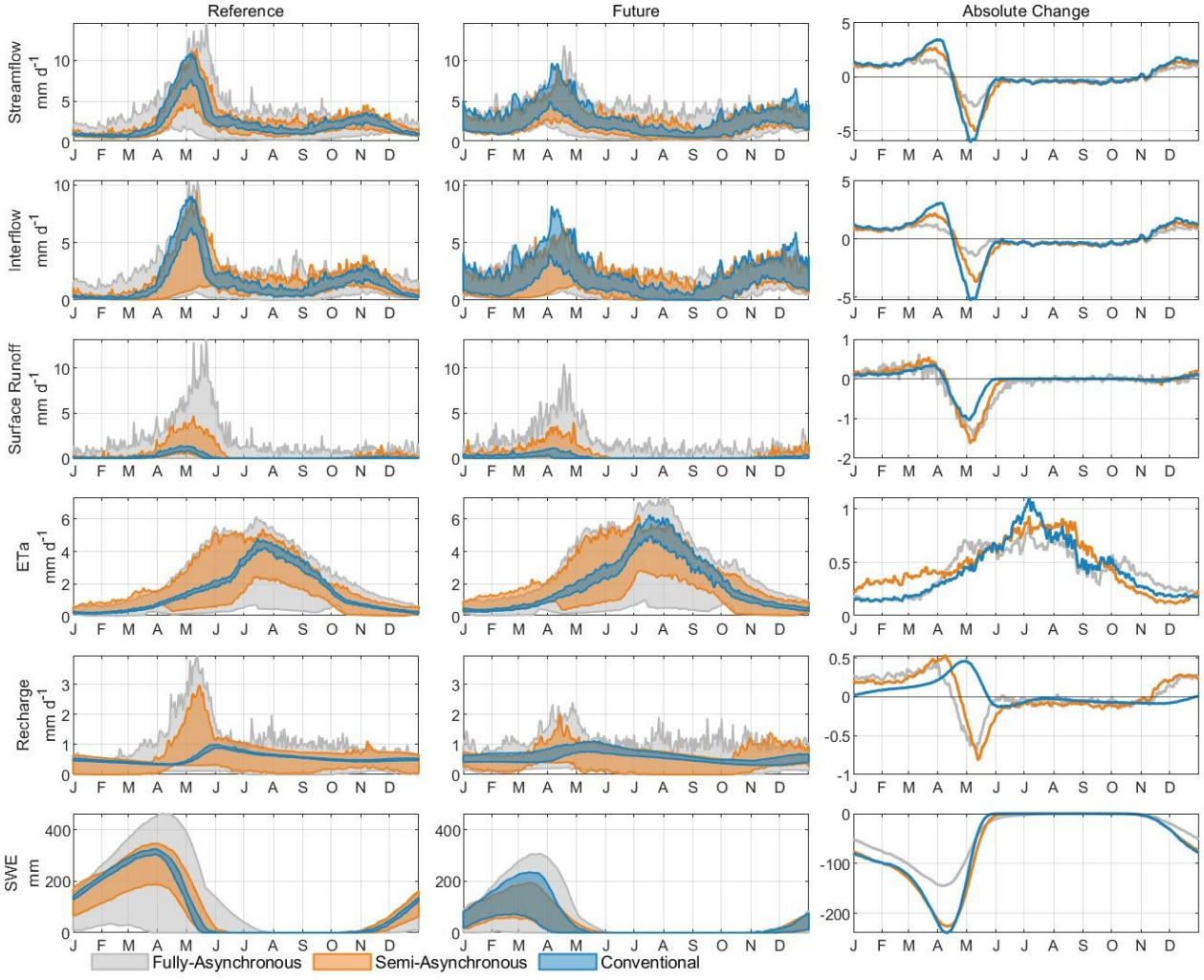

Figure F6. Same as F1, but for Bras du Nord catchment.

https://doi.org/10.5194/egusphere-2025-4450
Preprint. Discussion started: 18 September 2025

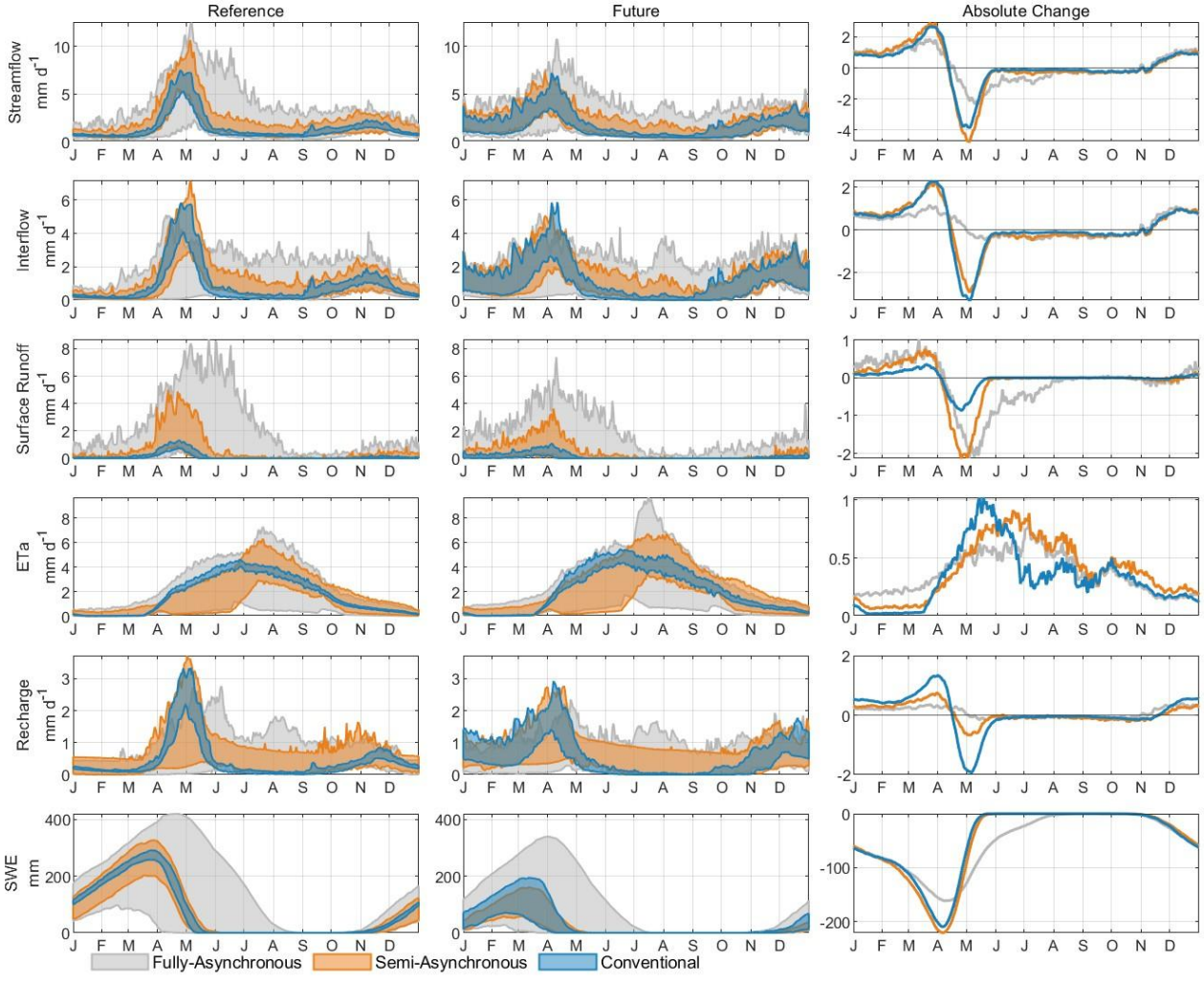

Figure F7. Same as F1, but for Du loup catchment.

https://doi.org/10.5194/egusphere-2025-4450
Preprint. Discussion started: 18 September 2025

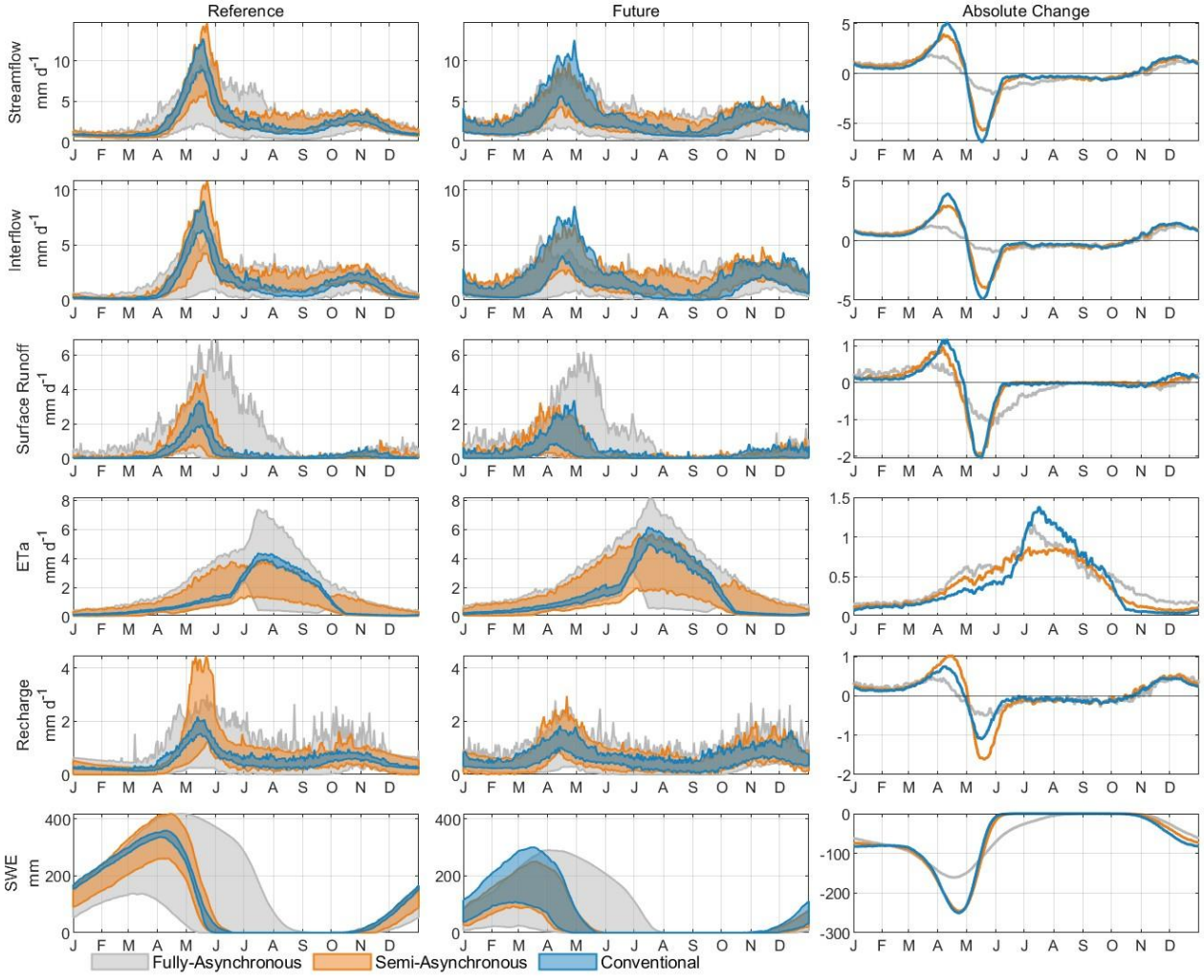

Figure F8. Same as F1, but for Valin catchment.

https://doi.org/10.5194/egusphere-2025-4450
Preprint. Discussion started: 18 September 2025

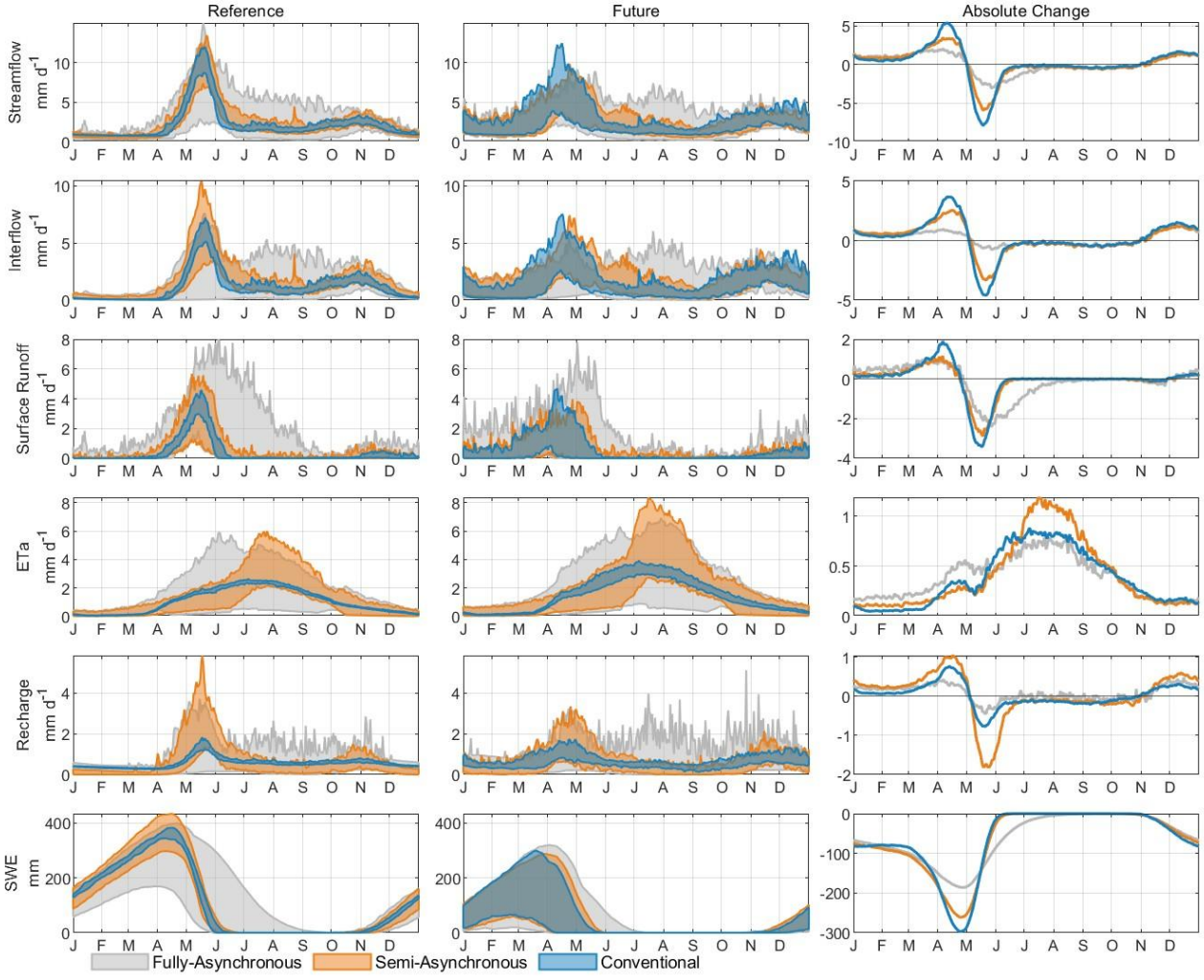

Figure F9. Same as F1, but for Godbout catchment.

Code and data availability

The calibrated WaSiM model and all simulations for all catchments discussed in this study is publicly accessible at https://osf.io/n87ey/ (Talbot et al., 2024b).

Author contribution

FT, JDS, SR, and RA contributed to the conceptualization and methodology design of the study. FT performed the formal analysis, investigation, data curation, and conducted the model simulations. JLM contributed to the MBCn post-processing of climate data ensembles. FT was responsible for visualization and led the original draft preparation. JDS and RA provided

https://doi.org/10.5194/egusphere-2025-4450
Preprint. Discussion started: 18 September 2025

supervision and project administration. AP, GD, JDS, RA, SR, JLM and FT contributed to the writing, review, and editing of the manuscript.

Competing interests

The authors declare that they have no conflict of interest.

Acknowledgements

This work was funded jointly by the Ministère des Ressources Naturelles et des Forêts (Quebec, Canada, project number 112332187 conducted at the Direction de la Recherche Forestière and led by Jean-Daniel Sylvain) and the Forest research service contract number 3322-2022-2187-01 obtained by Richard Arsenault from the Ministère des Ressources Naturelles et des Forêts (Quebec, Canada). The authors also acknowledge the use of ChatGPT-4 for assistance in correcting spelling mistakes and improving the flow of text during the manuscript preparation process. The base map in Fig. 1 was created using ArcGIS® software by Esri. ArcGIS® and ArcMap™ are the intellectual property of Esri and are used herein under license. Copyright © Esri. All rights reserved. For more information about Esri® software, please visit www.esri.com.

https://doi.org/10.5194/egusphere-2025-4450
Preprint. Discussion started: 18 September 2025

References

Arsenault, R., Brissette, F., Malo, J.-S., Minville, M., and Leconte, R.: Structural and Non-Structural Climate Change Adaptation Strategies for the Péribonka Water Resource System, Water Resour Manage, 27, 2075–2087, https://doi.org/10.1007/s11269-013-0275-6, 2013.

Arsenault, R., Poulin, A., Côté, P., and Brissette, F.: Comparison of Stochastic Optimization Algorithms in Hydrological Model Calibration, Journal of Hydrologic Engineering, 19, 1374–1384, https://doi.org/10.1061/(ASCE)HE.1943-5584.0000938, 2014.

Arsenault, R., Brissette, F., Chen, J., Guo, Q., and Dallaire, G.: NAC2H: The North American Climate Change and Hydroclimatology Data Set, Water Resources Research, 56, e2020WR027097, https://doi.org/10.1029/2020WR027097, 2020.

Arsenault, R., Huard, D., Martel, J.-L., Troin, M., Mai, J., Brissette, F., Jauvin, C., Vu, L., Craig, J. R., Smith, T. J., Logan, T., Tolson, B. A., Han, M., Gravel, F., and Langlois, S.: The PAVICS-Hydro platform: A virtual laboratory for hydroclimatic modelling and forecasting over North America, Environmental Modelling & Software, 168, 105808, https://doi.org/10.1016/j.envsoft.2023.105808, 2023.

Aygün, O., Kinnard, C., Campeau, S., and Pomeroy, J. W.: Landscape and climate conditions influence the hydrological sensitivity to climate change in eastern Canada, Journal of Hydrology, 615, 128595, https://doi.org/10.1016/j.jhydrol.2022.128595, 2022.

Beck, H. E., Zimmermann, N. E., McVicar, T. R., Vergopolan, N., Berg, A., and Wood, E. F.: Present and future Köppen-Geiger climate classification maps at 1-km resolution, Sci Data, 5, 180214, https://doi.org/10.1038/sdata.2018.214, 2018.

Bormann, H. and Elfert, S.: Application of WaSiM-ETH model to Northern German lowland catchments: model performance in relation to catchment characteristics and sensitivity to land use change, in: Advances in Geosciences, Hydrologic Modelling for the Assessment of Ecosystem Services and Landscape Functions - 3th Workshop “Large-scale Hydrological Modelling – Hydrological Modelling for the Assessment of Ecosystem Services and Landscape Functions”, Dresden, Germany, 25–27 November 2009, 1–10, https://doi.org/10.5194/adgeo-27-1-2010, 2010.

Calvin, K., Dasgupta, D., Krinner, G., Mukherji, A., Thorne, P. W., Trisos, C., Romero, J., Aldunce, P., Barrett, K., Blanco, G., Cheung, W. W. L., Connors, S., Denton, F., Diongue-Niang, A., Dodman, D., Garschagen, M., Geden, O., Hayward, B., Jones, C., Jotzo, F., Krug, T., Lasco, R., Lee, Y.-Y., Masson-Delmotte, V., Meinshausen, M., Mintenbeck, K., Mokssit, A., Otto, F. E. L., Pathak, M., Pirani, A., Poloczanska, E., Pörtner, H.-O., Revi, A., Roberts, D. C., Roy, J., Ruane, A. C., Skea, J., Shukla, P. R., Slade, R., Slangen, A., Sokona, Y., Sörensson, A. A., Tignor, M., Van Vuuren, D., Wei, Y.-M., Winkler, H., Zhai, P., Zommers, Z., Hourcade, J.-C., Johnson, F. X., Pachauri, S., Simpson, N. P., Singh, C., Thomas, A., Totin, E., Arias, P., Bustamante, M., Elgizouli, I., Flato, G., Howden, M., Méndez-Vallejo, C., Pereira, J. J., Pichs-Madruga, R., Rose, S. K., Saheb, Y., Sánchez Rodríguez, R., Ürge-Vorsatz, D., Xiao, C., Yassaa, N., Alegría, A., Armour, K., Bednar-Friedl, B., Blok, K., Cissé, G., Dentener, F., Eriksen, S., Fischer, E., Garner, G., Guivarch, C., Haasnoot, M., Hansen, G., Hauser, M., Hawkins, E., Hermans, T., Kopp, R., Leprince-Ringuet, N., Lewis, J., Ley, D., Ludden, C., Niamir, L., Nicholls, Z., Some, S., Szopa, S., Trewin, B., Van Der Wijst, K.-I., Winter, G., Witting, M., Birt, A., Ha, M., et al.: IPCC, 2023: Climate Change 2023: Synthesis Report. Contribution of Working Groups I, II and III to the Sixth Assessment Report of the Intergovernmental Panel on Climate Change [Core Writing Team, H. Lee and J. Romero (eds.)]. IPCC, Geneva, Switzerland., Intergovernmental Panel on Climate Change (IPCC), https://doi.org/10.59327/IPCC/AR6-9789291691647, 2023.

Cannon, A. J.: Multivariate quantile mapping bias correction: an N-dimensional probability density function transform for climate model simulations of multiple variables, Clim Dyn, 50, 31–49, https://doi.org/10.1007/s00382-017-3580-6, 2018.

https://doi.org/10.5194/egusphere-2025-4450
Preprint. Discussion started: 18 September 2025

Chen, J., Arsenault, R., Brissette, F. P., and Zhang, S.: Climate Change Impact Studies: Should We Bias Correct Climate Model Outputs or Post-Process Impact Model Outputs?, Water Resources Research, 57, e2020WR028638, https://doi.org/10.1029/2020WR028638, 2021.

2015 Land Cover of North America ar 30 meters: http://www.cec.org/north-american-environmental-atlas/land-cover-30m-2015-landsat-and-rapideye/, last access: 1 December 2023.

Conrad, O., Bechtel, B., Bock, M., Dietrich, H., Fischer, E., Gerlitz, L., Wehberg, J., Wichmann, V., and Böhner, J.: System for Automated Geoscientific Analyses (SAGA) v. 2.1.4, Geoscientific Model Development, 8, 1991–2007, https://doi.org/10.5194/gmd-8-1991-2015, 2015.

Devia, G. K., Ganasri, B. P., and Dwarakish, G. S.: A Review on Hydrological Models, Aquatic Procedia, 4, 1001–1007, https://doi.org/10.1016/j.aqpro.2015.02.126, 2015.

Estrada, F., Kim, D., and Perron, P.: Spatial variations in the warming trend and the transition to more severe weather in midlatitudes, Sci Rep, 11, 145, https://doi.org/10.1038/s41598-020-80701-7, 2021.

Farjad, B., Gupta, A., and Marceau, D. J.: Annual and Seasonal Variations of Hydrological Processes Under Climate Change Scenarios in Two Sub-Catchments of a Complex Watershed, Water Resour Manage, 30, 2851–2865, https://doi.org/10.1007/s11269-016-1329-3, 2016.

Förster, K., Meißl, G., Marke, T., Pohl, S., Garvelmann, J., Schulla, J., and Strasser, U.: A new snow-vegetation interaction extension for the Water Balance Simulation Model (WaSiM), 2620, 2017.

Förster, K., Garvelmann, J., Meißl, G., and Strasser, U.: Modelling forest snow processes with a new version of WaSiM, Hydrological Sciences Journal, 63, 1540–1557, https://doi.org/10.1080/02626667.2018.1518626, 2018.

van Genuchten, M. Th.: A Closed-form Equation for Predicting the Hydraulic Conductivity of Unsaturated Soils, Soil Science Society of America Journal, 44, 892–898, https://doi.org/10.2136/sssaj1980.03615995004400050002x, 1980.

Hersbach, H., Bell, B., Berrisford, P., Hirahara, S., Horányi, A., Muñoz-Sabater, J., Nicolas, J., Peubey, C., Radu, R., Schepers, D., Simmons, A., Soci, C., Abdalla, S., Abellan, X., Balsamo, G., Bechtold, P., Biavati, G., Bidlot, J., Bonavita, M., De Chiara, G., Dahlgren, P., Dee, D., Diamantakis, M., Dragani, R., Flemming, J., Forbes, R., Fuentes, M., Geer, A., Haimberger, L., Healy, S., Hogan, R. J., Hólm, E., Janisková, M., Keeley, S., Laloyaux, P., Lopez, P., Lupu, C., Radnoti, G., de Rosnay, P., Rozum, I., Vamborg, F., Villaume, S., and Thépaut, J.-N.: The ERA5 global reanalysis, Quarterly Journal of the Royal Meteorological Society, 146, 1999–2049, https://doi.org/10.1002/qj.3803, 2020.

Hydroclimatic Atlas of Southern Québec: https://www.cehq.gouv.qc.ca/atlas-hydroclimatique/index-en.htm, last access: 30 November 2023.

Jakob Themeßl, M., Gobiet, A., and Leuprecht, A.: Empirical-statistical downscaling and error correction of daily precipitation from regional climate models, International Journal of Climatology, 31, 1530–1544, https://doi.org/10.1002/joc.2168, 2011.

Jasper, K., Calanca, P., and Fuhrer, J.: Changes in summertime soil water patterns in complex terrain due to climatic change, Journal of Hydrology, 327, 550–563, https://doi.org/10.1016/j.jhydrol.2005.11.061, 2006.

Kling, H., Fuchs, M., and Paulin, M.: Runoff conditions in the upper Danube basin under an ensemble of climate change scenarios, Journal of Hydrology, 424–425, 264–277, https://doi.org/10.1016/j.jhydrol.2012.01.011, 2012.

https://doi.org/10.5194/egusphere-2025-4450
Preprint. Discussion started: 18 September 2025

Kour, R., Patel, N., and Krishna, A. P.: Climate and hydrological models to assess the impact of climate change on hydrological regime: a review, Arab J Geosci, 9, 544, https://doi.org/10.1007/s12517-016-2561-0, 2016.

Latifovic, R., Homer, C., Ressl, R., Pouliot, D. A., Hossian, S., Colditz, R., Olthof, I., Chandra, G., and Victoria, A.: North American Land Change Monitoring System, Remote Sensing of Land Use and Land Cover: Principles and Applications, 303–324, https://doi.org/10.1201/b11964-24, 2012.

Lee, M.-H., Lu, M., Im, E.-S., and Bae, D.-H.: Added value of dynamical downscaling for hydrological projections in the Chungju Basin, Korea, International Journal of Climatology, 39, 516–531, https://doi.org/10.1002/joc.5825, 2019.

Lucas-Picher, P., Lachance-Cloutier, S., Arsenault, R., Poulin, A., Ricard, S., Turcotte, R., and Brissette, F.: Will Evolving Climate Conditions Increase the Risk of Floods of the Large U.S.-Canada Transboundary Richelieu River Basin?, JAWRA Journal of the American Water Resources Association, 57, 32–56, https://doi.org/10.1111/1752-1688.12891, 2021.

Ludwig, R., May, I., Turcotte, R., Vescovi, L., Braun, M., Cyr, J.-F., Fortin, L.-G., Chaumont, D., Biner, S., Chartier, I., Caya, D., and Mauser, W.: The role of hydrological model complexity and uncertainty in climate change impact assessment, Advances in Geosciences, 21, 63–71, https://doi.org/10.5194/adgeo-21-63-2009, 2009.

Mei, Y., Mai, J., Do, H. X., Gronewold, A., Reeves, H., Eberts, S., Niswonger, R., Regan, R. S., and Hunt, R. J.: Can Hydrological Models Benefit From Using Global Soil Moisture, Evapotranspiration, and Runoff Products as Calibration Targets?, Water Resources Research, 59, e2022WR032064, https://doi.org/10.1029/2022WR032064, 2023.

Milly, P. C. D., Dunne, K. A., and Vecchia, A. V.: Global pattern of trends in streamflow and water availability in a changing climate, Nature, 438, 347–350, https://doi.org/10.1038/nature04312, 2005.

Ministère des Ressources Naturelles et des Forêts: SIIGSOL-100m - Carte des propriétés du sol, Données Québec, 2022.

Minville, M., Brissette, F., and Leconte, R.: Uncertainty of the impact of climate change on the hydrology of a nordic watershed, Journal of Hydrology, 358, 70–83, https://doi.org/10.1016/j.jhydrol.2008.05.033, 2008.

Moges, E., Demissie, Y., Larsen, L., and Yassin, F.: Review: Sources of Hydrological Model Uncertainties and Advances in Their Analysis, Water, 13, 28, https://doi.org/10.3390/w13010028, 2021.

Mpelasoka, F. S. and Chiew, F. H. S.: Influence of Rainfall Scenario Construction Methods on Runoff Projections, https://doi.org/10.1175/2009JHM1045.1, 2009.

Natkhin, M., Steidl, J., Dietrich, O., Dannowski, R., and Lischeid, G.: Differentiating between climate effects and forest growth dynamics effects on decreasing groundwater recharge in a lowland region in Northeast Germany, Journal of Hydrology, 448–449, 245–254, https://doi.org/10.1016/j.jhydrol.2012.05.005, 2012.

Nolin, A. F., Girardin, M. P., Adamowski, J. F., Barzegar, R., Boucher, M.-A., Tardif, J. C., and Bergeron, Y.: Observed and projected trends in spring flood discharges for the Upper Harricana River, eastern boreal Canada, Journal of Hydrology: Regional Studies, 48, 101462, https://doi.org/10.1016/j.ejrh.2023.101462, 2023.

O'Neill, B. C., Tebaldi, C., van Vuuren, D. P., Eyring, V., Friedlingstein, P., Hurtt, G., Knutti, R., Kriegler, E., Lamarque, J.-F., Lowe, J., Meehl, G. A., Moss, R., Riahi, K., and Sanderson, B. M.: The Scenario Model Intercomparison Project (ScenarioMIP) for CMIP6, Geoscientific Model Development, 9, 3461–3482, https://doi.org/10.5194/gmd-9-3461-2016, 2016.

Piani, C., Haerter, J. O., and Coppola, E.: Statistical bias correction for daily precipitation in regional climate models over Europe, Theor Appl Climatol, 99, 187–192, https://doi.org/10.1007/s00704-009-0134-9, 2010.

Poulin, A., Brissette, F., Leconte, R., Arsenault, R., and Malo, J.-S.: Uncertainty of hydrological modelling in climate change impact studies in a Canadian, snow-dominated river basin, Journal of Hydrology, 409, 626–636, https://doi.org/10.1016/j.jhydrol.2011.08.057, 2011.

Ricard, S., Sylvain, J.-D., and Anctil, F.: Exploring an Alternative Configuration of the Hydroclimatic Modeling Chain, Based on the Notion of Asynchronous Objective Functions, Water, 11, 2012, https://doi.org/10.3390/w11102012, 2019.

Ricard, S., Sylvain, J.-D., and Anctil, F.: Asynchronous Hydroclimatic Modeling for the Construction of Physically Based Streamflow Projections in a Context of Observation Scarcity, Frontiers in Earth Science, 8, 2020.

Ricard, S., Lucas-Picher, P., Thiboult, A., and Anctil, F.: Producing reliable hydrologic scenarios from raw climate model outputs without resorting to meteorological observations, Hydrology and Earth System Sciences, 27, 2375–2395, https://doi.org/10.5194/hess-27-2375-2023, 2023.

Richards, L. A.: CAPILLARY CONDUCTION OF LIQUIDS THROUGH POROUS MEDIUMS, Physics, 1, 318–333, https://doi.org/10.1063/1.1745010, 1931.

WaSiM-ETH Documentation: http://www.wasim.ch/en/products/wasim_description.htm, last access: 30 November 2023.

Sivakumar, B.: Global climate change and its impacts on water resources planning and management: assessment and challenges, Stoch Environ Res Risk Assess, 25, 583–600, https://doi.org/10.1007/s00477-010-0423-y, 2011.

Sylvain, J.-D., Anctil, F., and Thiffault, E.: Using bias correction and ensemble modelling for predictive mapping and related uncertainty: A case study in digital soil mapping, Geoderma, 403, 1–29, https://doi.org/10.1016/j.geoderma.2021.115153, 2021.

T. W. Chu and A. Shirmohammadi: EVALUATION OF THE SWAT MODELS HYDROLOGY COMPONENT IN THE PIEDMONT PHYSIOGRAPHIC REGION OF MARYLAND, Transactions of the ASAE, 47, 1057–1073, https://doi.org/10.13031/2013.16579, 2004.

Talbot, F., Sylvain, J.-D., Drolet, G., Poulin, A., and Arsenault, R.: Enhancing physically based and distributed hydrological model calibration through internal state variable constraints, EGUsphere, 1–42, https://doi.org/10.5194/egusphere-2024-3353, 2024a.

Talbot, F., Ricard, S., Sylvain, J.-D., Drolet, G., Poulin, A., and Arsenault, R.: HESS paper data - Wasim Semi-Asynchronous climate change impact modelling, https://doi.org/10.17605/OSF.IO/N87EY, 2024b.

Talbot, F., Sylvain, J.-D., Drolet, G., Poulin, A., Martel, J.-L., and Arsenault, R.: Assessing hydroclimatic impacts of climate change in snowy catchments using a physically based hydrological model, Journal of Hydrology: Regional Studies, 59, 102453, https://doi.org/10.1016/j.ejrh.2025.102453, 2025.

Tarek, M., Brissette, F. P., and Arsenault, R.: Evaluation of the ERA5 reanalysis as a potential reference dataset for hydrological modelling over North America, Hydrology and Earth System Sciences, 24, 2527–2544, https://doi.org/10.5194/hess-24-2527-2020, 2020.

https://doi.org/10.5194/egusphere-2025-4450
Preprint. Discussion started: 18 September 2025

Tarek, M., Brissette, F., and Arsenault, R.: Uncertainty of gridded precipitation and temperature reference datasets in climate change impact studies, Hydrology and Earth System Sciences, 25, 3331–3350, https://doi.org/10.5194/hess-25-3331-2021, 2021.

Tolson, B. A. and Shoemaker, C. A.: Dynamically dimensioned search algorithm for computationally efficient watershed model calibration, Water Resources Research, 43, https://doi.org/10.1029/2005WR004723, 2007.

Valencia Giraldo, M. del C., Ricard, S., and Anctil, F.: Assessment of the Potential Hydrological Impacts of Climate Change in Quebec—Canada, a Refined Neutral Approach, Water, 15, 584, https://doi.org/10.3390/w15030584, 2023.

Yassin, F., Razavi, S., Wheater, H., Sapriza-Azuri, G., Davison, B., and Pietroniro, A.: Enhanced identification of a hydrologic model using streamflow and sat ellite water storage data: A multicriteria sensitivity analysis and op timization approach, Hydrological Processes, 31, 3320–3333, https://doi.org/10.1002/hyp.11267, 2017.